Acta Math Vietnam (2018) 43:503–547
https://doi.org/10.1007/s40306-017-0242-z

A van Leer-Type Numerical Scheme for the Model of a General Fluid Flow in a Nozzle with Variable Cross Section

Mai Duc Thanh[1] · **Dao Huy Cuong**[2,3]

Received: 26 April 2017 / Revised: 4 October 2017 / Accepted: 11 October 2017 /
Published online: 29 December 2017

Abstract A van Leer-type numerical scheme for the model of a general fluid in a nozzle with variable cross section is presented. The model is nonconservative, making it hard for standard numerical schemes. Exact solutions of local Riemann problems are incorporated in the construction of this scheme. The scheme can work well in regions of resonance, where multiple waves are colliding. Numerical tests are conducted, where we compare the errors and orders of accuracy for approximating exact solutions between this scheme and a Godunov-type scheme. Results from numerical tests show that this van Leer-type scheme has a much better accuracy than the Godunov-type scheme.

Keywords Numerical approximation · van Leer-type scheme · Fluid · Nozzle · Shock · Nonconservative · Riemann solver

Mathematics Subject Classification (2010) 35L65 · 65M06 · 76T10

✉ Mai Duc Thanh
mdthanh@hcmiu.edu.vn

Dao Huy Cuong
cuongnhc82@gmail.com

[1] Department of Mathematics, International University (VNU-HCM), Quarter 6, Linh Trung Ward, Thu Duc District, Ho Chi Minh City, Vietnam

[2] Nguyen Huu Cau High School, 07 Nguyen Anh Thu, Trung Chanh Ward, Hoc Mon District, Ho Chi Minh City, Vietnam

[3] Department of Mathematics and Computer Science, University of Science (VNU-HCM), 227 Nguyen Van Cu Str., District 5, Ho Chi Minh City, Vietnam

1 Introduction

In this paper, we build a van Leer-type scheme for approximating solutions of the following model of a general fluid flow in a nozzle with variable cross section

$$\begin{aligned} &\partial_t(a\rho) + \partial_x(a\rho u) = 0,\\ &\partial_t(a\rho u) + \partial_x\Big(a(\rho u^2 + p)\Big) = p\partial_x a,\\ &\partial_t(a\rho e) + \partial_x\left(au(\rho e + p)\right) = 0, \quad x \in \boldsymbol{R}, t > 0, \end{aligned} \tag{1.1}$$

where $\rho = \rho(x,t)$, $\varepsilon = \varepsilon(x,t)$, $T = T(x,t)$, $S = S(x,t)$, and $p = p(x,t)$ denote the thermodynamic variables: density, internal energy, absolute temperature, specific entropy, and the pressure, respectively; $u = u(x,t)$ is the velocity; $e = e(x,t) = \varepsilon + u^2/2$ is the total energy; and $a = a(x) > 0$, $x \in \mathbb{R}$ is the cross-sectional area.

The model (1.1) contains a nonconservative source term. To deal with this obstacle, one often supplements the system (1.1) with the trivial equation

$$\partial_t a = 0, \tag{1.2}$$

and then, the system (1.1)–(1.2) can be re-written as a system of balance laws in nonconservative form. A formulation of weak solutions of this kind of systems was introduced in [16]. Numerical approximating nonconservative systems of balance laws is a challenging topic during the past decades. Often, nonconservative terms cause serious problems to standard schemes. For example, errors may not tend to zero when the mesh sizes tend to zero, or even numerical oscillations may appear quickly.

Motivated by our recent work [14], we will construct a van Leer-type scheme for (1.1). Note that in the literature, the second-order van Leer scheme can be seen as an important improvement of the first-order Godunov scheme for hyperbolic conservation laws. Therefore, we will also show that this van Leer-type scheme can provide us with a better accuracy than the Godunov-type scheme. It is interesting that this van Leer-type scheme can also give good approximations in the resonance cases where the exact solution contains several waves associated with different characteristic fields with coinciding shock speeds.

Throughout, we assume for simplicity that the fluid is polytropic and ideal so that the equation of state is given by

$$p = (\gamma - 1)\rho\varepsilon, \tag{1.3}$$

where $\gamma > 1$ is the adiabatic exponent.

We note that there are many works in the literature for the study on nonconservative systems of balance laws. Theoretical studies on nonconservative systems of balance laws were presented in [19, 20, 23–25, 27, 32–34]. Numerical treatments for balance laws in nonconservative form were studied in [7–9, 18]. Numerical schemes for shallow-water equations were considered in [3, 6, 13, 26, 28]. Numerical schemes for the model of a fluid flow in a nozzle with variable cross section were constructed in [5, 11, 15, 21, 22]. Generalized Riemann problems were considered in [4]. Numerical schemes for two-phase flow models were presented in [1, 2, 10, 12, 29–31]. The reader is referred to [17] for standard numerical schemes for hyperbolic systems of conservation laws (see also the references therein).

The organization of this paper is as follows. Basic properties of the model (1.1)–(1.2) are given in Section 2. In Section 3, the Riemann problem is revisited. Section 4 is devoted to the construction of the van Leer-type scheme for (1.1). Numerical tests are given in Section 5, where we compute the errors and orders of accuracy. Finally, we present several conclusions in Section 6.

2 Preliminaries

2.1 Nonstrict Hyperbolic Model

Using the thermodynamical identity, we can express the pressure p from (1.3) as a function of the density ρ and the specific entropy S

$$p = p(\rho, S) = \kappa(S)\rho^{\gamma}, \quad \kappa(S) = (\gamma - 1)\exp\left(\frac{S - S_*}{C_{\mathrm{v}}}\right), \tag{2.1}$$

where $C_{\mathrm{v}} > 0$ is the specific heat at constant volume and S_* is constant. Note that for a polytropic and ideal fluid, γ and C_{v} are constants.

Thus, if we choose (p, S) as two independent thermodynamic variables, we can write

$$\rho = \rho(p, S) = \left(\frac{p}{\kappa(S)}\right)^{1/\gamma}. \tag{2.2}$$

Therefore, for a smooth solution $U = U(x,t) = (p(x,t), u(x,t), S(x,t), a(x))^T$, the system (1.1) can be re-written as a system of balance laws in nonconservative form

$$\partial_t U + \mathbf{A}(U)\partial_x U = 0, \tag{2.3}$$

where

$$\mathbf{A}(U) = \begin{pmatrix} u & \rho c^2 & 0 & \rho u c^2/a \\ 1/\rho & u & 0 & 0 \\ 0 & 0 & u & 0 \\ 0 & 0 & 0 & 0 \end{pmatrix}, \tag{2.4}$$

where c is the sound speed,

$$c^2 = \frac{\gamma p}{\rho}. \tag{2.5}$$

The characteristic equation is given by

$$\lambda(u - \lambda)\left((u - \lambda)^2 - c^2\right) = 0.$$

Thus, we obtain four real eigenvalues

$$\lambda_0(U) = 0, \quad \lambda_1(U) = u - c, \quad \lambda_2(U) = u, \quad \lambda_3(U) = u + c. \tag{2.6}$$

The corresponding eigenvectors can be chosen as

$$r_0(U) = \left(-\rho u^2 c^2, uc^2, 0, a(u^2 - c^2)\right)^T, \quad r_1(U) = (\rho c, -1, 0, 0)^T,$$
$$r_2(U) = (0, 0, 1, 0)^T, \quad r_3(U) = (\rho c, 1, 0, 0)^T.$$

Therefore, the system (1.1) is hyperbolic, but not strictly hyperbolic. More precisely, λ_0 and λ_1 coincide on the hypersurface

$$\mathcal{C}^+ = \{U : u = c\}.$$

λ_0 and λ_2 coincide on the hypersurface

$$\mathcal{C}^0 = \{U : u = 0\}.$$

λ_0 and λ_3 coincide on the hypersurface

$$\mathcal{C}^- = \{U : u = -c\}.$$

These surfaces, referred to as *strictly hyperbolic boundaries*, separate the phase domain into four subdomains, denoted by G_1^+, G_2^+, G_2^-, and G_1^-, in which the system is strictly hyperbolic (see Fig. 1).

$$\begin{aligned} G_1^+ &= \{U : \lambda_0(U) < \lambda_1(U)\}, \\ G_2^+ &= \{U : \lambda_1(U) < \lambda_0(U) < \lambda_2(U)\}, \\ G_2^- &= \{U : \lambda_2(U) < \lambda_0(U) < \lambda_3(U)\}, \\ G_1^- &= \{U : \lambda_3(U) < \lambda_0(U)\}. \end{aligned} \tag{2.7}$$

The second and the zero characteristic fields are *linearly degenerate*, since

$$\nabla\lambda_0(U) \cdot r_0(U) = \nabla\lambda_2(U) \cdot r_2(U)0.$$

The first and the third characteristic fields are *genuinely nonlinear*, since

$$-\nabla\lambda_1(U) \cdot r_1(U) = \nabla\lambda_3(U) \cdot r_3(U) = \frac{\gamma+1}{2} > 0.$$

2.2 Rarefaction Waves

The k-rarefaction waves of the system (1.1) are the continuous piecewise-smooth self-similar weak solutions of (1.1) associated with nonlinear characteristic fields (λ_k, r_k), $k = 1, 3$, which have the form

$$U(x,t) = \begin{cases} U_-, & x/t < \lambda_k(U_-), \\ \text{Fan}_k(x/t; U_-, U_+), & \lambda_k(U_-) \le x/t \le \lambda_k(U_+), \\ U_+, & x/t > \lambda_k(U_+), \end{cases} \tag{2.8}$$

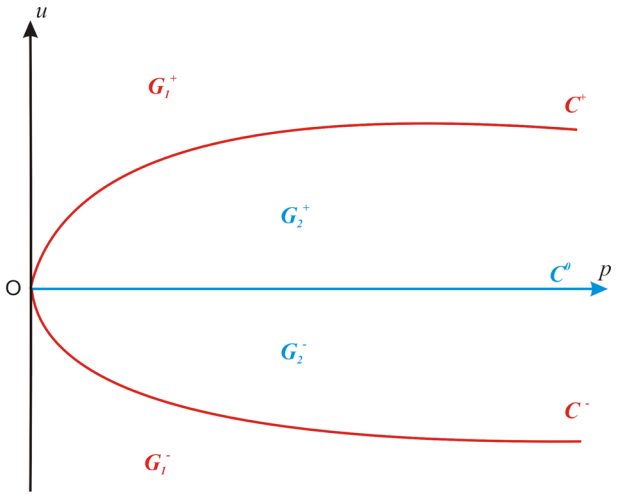

Fig. 1 Hyperbolic boundaries and the four phases in the $(p, u)-$plane

where $V(\xi) := \mathrm{Fan}_k(\xi; U_-, U_+)$ is a solution of the following ordinary differential equations

$$\begin{aligned} &\frac{dV(\xi)}{d\xi} = \frac{1}{\nabla\lambda_k(V(\xi))\cdot r_k(V(\xi))} r_k(V(\xi)), \quad \lambda_k(U_-) \le \xi \le \lambda_k(U_+), \\ &V(\lambda_k(U_\pm)) = U_\pm. \end{aligned} \tag{2.9}$$

For $k = 1$, we determine $V(\xi) = (p(\xi), u(\xi), S(\xi), a(\xi))$ from (2.9) as follows

$$\begin{aligned} \frac{dp}{d\xi} &= -\frac{2}{\gamma+1}\rho c, \\ \frac{du}{d\xi} &= \frac{2}{\gamma+1}, \\ \frac{dS}{d\xi} &= \frac{da}{d\xi} = 0, \end{aligned} \tag{2.10}$$

or, equivalently,

$$\begin{aligned} &S(\xi) = S_- = S_+, \\ &a(\xi) = a_- = a_+, \\ &p(\xi) = \left(p_-^{\frac{\gamma-1}{2\gamma}} - \frac{\gamma-1}{\sqrt{\gamma}(\gamma+1)} (\kappa(S_-))^{-\frac{1}{2\gamma}} (\xi - \lambda_1(U_-)) \right)^{\frac{2\gamma}{\gamma-1}}, \\ &u(\xi) = u_- + \frac{2}{\gamma+1}(\xi - \lambda_1(U_-)). \end{aligned}$$

From (2.10), the *forward* 1-rarefaction wave curve $\mathcal{R}_1(U_0)$ consisting of all right-hand states $U = (p, u, \rho, a)$ that can be connected to a given left-hand state $U_0 = (p_0, u_0, \rho_0, a_0)$ by an 1-rarefaction wave is given by

$$\begin{aligned} \mathcal{R}_1(U_0): \quad & a = a_0, \\ & \left(\frac{\rho}{\rho_0}\right)^\gamma = \frac{p}{p_0}, \\ & u = u_0 - \frac{2\sqrt{\gamma}}{\gamma-1} (\kappa(S_0))^{\frac{1}{2\gamma}} \left(p^{\frac{\gamma-1}{2\gamma}} - p_0^{\frac{\gamma-1}{2\gamma}} \right), \quad p \le p_0. \end{aligned} \tag{2.11}$$

Similarly, for $k = 3$, we have

$$\begin{aligned} &S(\xi) = S_- = S_+, \\ &a(\xi) = a_- = a_+, \\ &p(\xi) = \left(p_-^{\frac{\gamma-1}{2\gamma}} + \frac{\gamma-1}{\sqrt{\gamma}(\gamma+1)} (\kappa(S_-))^{-\frac{1}{2\gamma}} (\xi - \lambda_3(U_-)) \right)^{\frac{2\gamma}{\gamma-1}}, \\ &u(\xi) = u_- + \frac{2}{\gamma+1}(\xi - \lambda_3(U_-)). \end{aligned}$$

Therefore, the *backward* 3-rarefaction wave curve $\mathcal{R}_3^B(U_0)$ consisting of all left-hand states $U = (p, u, \rho, a)$ that can be connected to a given right-hand state $U_0 = (p_0, u_0, \rho_0, a_0)$ by an 3-rarefaction wave is given by

$$\begin{aligned} \mathcal{R}_3^B(U_0): \quad & a = a_0, \\ & \left(\frac{\rho}{\rho_0}\right)^{\gamma} = \frac{p}{p_0}, \\ & u = u_0 + \frac{2\sqrt{\gamma}}{\gamma - 1}(\kappa(S_0))^{\frac{1}{2\gamma}} \left(p^{\frac{\gamma-1}{2\gamma}} - p_0^{\frac{\gamma-1}{2\gamma}}\right), \quad p \le p_0 \end{aligned} \tag{2.12}$$

2.3 Shocks and Admissibility Criterion

A discontinuity wave of (1.1) is a weak solution of the form

$$U(x,t) = \begin{cases} U_-, & x < \sigma t, \\ U_+, & x > \sigma t, \end{cases} \tag{2.13}$$

where U_-, U_+ are left- and right-hand states, respectively, and σ is the shock speed.

A shock wave always satisfies the Rankine-Hugoniot relation for the conservative equation $\partial_t a = 0$, which reads

$$-\sigma[a] = 0.$$

The last relation leads to the following two cases:

(i) either the cross section remained unchanged across the shock, i.e., $[a] = 0$, or
(ii) the shock speed vanishes:

$$\sigma = 0.$$

If $[a] = 0$, then, the cross section is constant across the shock. We can eliminate this constant value in the governing equations (1.1) and obtain the usual gas dynamics equations. Thus, the Rankine-Hugoniot relations for the shock are given by

$$\begin{aligned} & -\sigma[\rho] + [\rho u] = 0, \\ & -\sigma[\rho u] + [\rho u^2 + p] = 0, \\ & -\sigma[\rho e] + [u(\rho e + p)] = 0. \end{aligned} \tag{2.14}$$

Transforming the relations (2.14) yields

$$\begin{aligned} & M := \rho_+(u_+ - \sigma) = \rho_-(u_- - \sigma), \\ & \rho_+(u_+ - \sigma)^2 + p_+ = \rho_-(u_- - \sigma)^2 + p_-, \\ & (u_+ - \sigma)\left(\rho_+\left(\varepsilon_+ + \frac{1}{2}(u_+ - \sigma)^2\right) + p_+\right) = (u_- - \sigma)\left(\rho_-\left(\varepsilon_- + \frac{1}{2}(u_- - \sigma)^2\right) + p_-\right). \end{aligned} \tag{2.15}$$

If $M = 0$, then,

$$\begin{aligned} & \sigma = u_+ = u_-, \\ & p_+ = p_-. \end{aligned}$$

Thus, in this case, the discontinuity wave (2.13) is called the 2-contact discontinuity corresponding to the shock speed $\sigma_2(U_-, U_+) = u_\pm = \lambda_2(U_\pm)$.

If $M \neq 0$, then, the relations (2.15) can be equivalently written

$$\begin{aligned} M &= \frac{u_+ - u_-}{\frac{1}{\rho_+} - \frac{1}{\rho_-}}, \\ M^2 &= -\frac{p_+ - p_-}{\frac{1}{\rho_+} - \frac{1}{\rho_-}}, \\ \varepsilon_+ - \varepsilon_- &+ \frac{1}{2}(p_+ + p_-)\left(\frac{1}{\rho_+} - \frac{1}{\rho_-}\right) = 0. \end{aligned} \tag{2.16}$$

Then, we obtain

$$\begin{aligned} \frac{\rho_+}{\rho_-} &= \frac{(\gamma+1)p_+ + (\gamma-1)p_-}{(\gamma+1)p_- + (\gamma-1)p_+}, \\ u_+ - u_- &= \pm\sqrt{-(p_+ - p_-)\left(\frac{1}{\rho_+} - \frac{1}{\rho_-}\right)}. \end{aligned} \tag{2.17}$$

Shock waves associated with nonlinear characteristic fields, as indicated above, are required to fulfill the Lax shock inequalities

$$\lambda_i(U_+) < \sigma(U_-, U_+) < \lambda_i(U_-), \quad i = 1, 3. \tag{2.18}$$

Observe that for a polytropic ideal gas (1.3), shock waves satisfying the Lax shock inequalities (2.18) are characterized as follows.

(a) For a 1-Lax shock,

$$M > 0, \quad u_+ < u_-, \quad p_+ > p_-. \tag{2.19}$$

(b) For a 3-Lax shock,

$$M < 0, \quad u_- > u_+, \quad p_- > p_+. \tag{2.20}$$

From (2.18) and (2.19), the *forward* 1-shock wave curve $\mathcal{S}_1(U_0)$ consisting of all right-hand states $U = (p, u, \rho, a)$ that can be connected to a given left-hand state $U_0 = (p_0, u_0, \rho_0, a_0)$ by an 1-Lax shock wave is given by

$$\begin{aligned} \mathcal{S}_1(U_0): \quad & a = a_0, \\ & \frac{\rho}{\rho_0} = \frac{(\gamma+1)p + (\gamma-1)p_0}{(\gamma+1)p_0 + (\gamma-1)p}, \\ & u - u_0 = -\sqrt{-(p - p_0)\left(\frac{1}{\rho} - \frac{1}{\rho_0}\right)}, \quad p \geq p_0. \end{aligned} \tag{2.21}$$

From (2.18) and (2.20), the *backward* 3-shock wave curve $\mathcal{S}_3^B(U_0)$ consisting of all left-hand states $U = (p, u, \rho, a)$ that can be connected to a given right-hand state $U_0 = (p_0, u_0, \rho_0, a_0)$ by an 3-Lax shock wave is given by

$$\begin{aligned} \mathcal{S}_1(U_0): \quad & a = a_0, \\ & \frac{\rho}{\rho_0} = \frac{(\gamma+1)p + (\gamma-1)p_0}{(\gamma+1)p_0 + (\gamma-1)p}, \\ & u - u_0 = \sqrt{-(p - p_0)\left(\frac{1}{\rho} - \frac{1}{\rho_0}\right)}, \quad p \geq p_0. \end{aligned} \tag{2.22}$$

For $U_R \in \mathcal{S}_1(U_L)$, we have the 1-shock speed

$$\sigma_1(U_L, U_R) = u_L - \sqrt{\frac{(\gamma+1)p_R + (\gamma-1)p_L}{2\rho_L}}, \quad p_R > p_L. \tag{2.23}$$

For $U_L \in \mathcal{S}_3^B(U_R)$, we have the 3-shock speed

$$\sigma_3(U_L, U_R) = u_R + \sqrt{\frac{(\gamma+1)p_L + (\gamma-1)p_R}{2\rho_R}}, \quad p_L > p_R. \tag{2.24}$$

From (2.23) and (2.24), we have the following lemma.

Lemma 2.1 ([32, Proposition 3.3])
1. *The 1-shock speed $\sigma_1(U_0, U)$ may change sign along the forward 1-shock wave curve $\mathcal{S}_1(U_0)$. More precisely, we have the following:*
(i) *If $U_0 \in G_2^+ \cup G_2^- \cup G_1^-$, then $\sigma_1(U_0, U)$ remains negative:*

$$\sigma_1(U_0, U) < 0, \quad U \in \mathcal{S}_1(U_0). \tag{2.25}$$

(ii) *If $U_0 \in G_1^+$, then $\sigma_1(U_0, U)$ vanishes once at some point $U = U^\# \in \mathcal{G}_2^+$ corresponding to a value*

$$p = p^\# = \frac{2\rho_0 u_0^2 - (\gamma-1)p_0}{\gamma+1} \tag{2.26}$$

on the forward 1-shock wave curve $\mathcal{S}_1(U_0)$ such that

$$\begin{aligned} &\sigma_1(U_0, U^\#) = 0, \\ &\sigma_1(U_0, U) > 0, \quad p \in (p_0, p^\#), \\ &\sigma_1(U_0, U) < 0, \quad p > p^\#. \end{aligned}$$

2. *The 3-shock speed $\sigma_3(U, U_0)$ may change sign along the backward 3-shock wave curve $\mathcal{S}_3^B(U_0)$. More precisely, we have the following:*
(i) *If $U_0 \in G_1^+ \cup G_2^+ \cup G_2^-$, then $\sigma_3(U, U_0)$ remains positive:*

$$\sigma_3(U, U_0) > 0, \quad U \in \mathcal{S}_3^B(U_0). \tag{2.27}$$

(ii) *If $U_0 \in G_1^-$, then $\sigma_3(U, U_0)$ vanishes once at some point $U = U^@ \in G_2^-$ corresponding to a value*

$$p = p^@ = \frac{2\rho_0 u_0^2 - (\gamma-1)p_0}{\gamma+1} \tag{2.28}$$

on the backward 3-shock wave curve $\mathcal{S}_3^B(U_0)$ such that

$$\begin{aligned} &\sigma_3(U^@, U_0) = 0, \\ &\sigma_3(U, U_0) < 0, \quad p \in (p_0, p^@), \\ &\sigma_3(U, U_0) > 0, \quad p > p^@. \end{aligned}$$

Moreover, since $\sigma_1(U_-, U_+) = u_- - \frac{M}{\rho_-} = u_+ - \frac{M}{\rho_+}$ and $M > 0$, we imply that

$$\sigma_1(U_-, U_+) < \lambda_2(U_\pm).$$

Similarly, it holds that

$$\sigma_3(U_-, U_+) > \lambda_2(U_\pm).$$

From (2.11), (2.12), (2.21), and (2.22), we can therefore define the forward and backward wave curves in the nonlinear characteristic fields as follows.

$$\begin{aligned} \mathcal{W}_1(U_0) &:= \mathcal{S}_1(U_0) \cup \mathcal{R}_1(U_0), \\ \mathcal{W}_3^B(U_0) &:= \mathcal{S}_3^B(U_0) \cup \mathcal{R}_3^B(U_0). \end{aligned} \tag{2.29}$$

These sets mean that:

• If $U_+ \in \mathcal{W}_1(U_-)$, then there is the 1-wave (1-rarefaction wave or 1-shock wave) connecting U_- to U_+, denoted by

$$W_1(U_-, U_+) \quad (R_1(U_-, U_+) \quad \text{or} \quad S_1(U_-, U_+).$$

• If $U_- \in \mathcal{W}_3^B(U_+)$, then there is the 3-wave (3-rarefaction wave or 3-shock wave) connecting U_- to U_+, denoted by

$$W_3(U_-, U_+) \quad (R_3(U_-, U_+) \quad \text{or} \quad S_3(U_-, U_+).$$

2.4 Stationary Waves

Consider the case

$$\sigma = 0 = \lambda_0.$$

This means that the shock wave is a contact wave associated with λ_0. As shown in [32], the jump relations for this contact wave are given by

$$\begin{aligned} &[a\rho u] = 0, \\ &\left[\frac{u^2}{2} + h\right] = 0, \\ &[S] = 0, \end{aligned} \tag{2.30}$$

where h is *specific enthalpy* given by

$$h = \varepsilon + \frac{p}{\rho} = \frac{c^2}{\gamma - 1},$$

We now describe the set of states U which can be connected to a given state U_0 by a stationary contact wave (associated with λ_0), where the cross section levels on both sides a_0 and a are considered to be fixed. Substituting $u = \frac{a_0\rho_0 u_0}{a\rho}$ from the 1st equation of (2.30) into the 3rd equation of (2.30), we obtain the nonlinear equation

$$F(\rho) := -\frac{2\gamma\kappa(S_0)}{\gamma - 1}\rho^{\gamma+1} + \left(u_0^2 + \frac{2\gamma\kappa(S_0)}{\gamma - 1}\rho_0^{\gamma-1}\right)\rho^2 - \left(\frac{a\rho_0 u_0}{a}\right)^2 = 0. \tag{2.31}$$

The domain of the function $F(\rho)$ is given by

$$\rho \le \overline{\rho} := \left(\frac{\gamma - 1}{2\gamma\kappa(S_0)}u_0^2 + \rho_0^{\gamma-1}\right)^{\frac{1}{\gamma-1}}.$$

Consider the case $u_0 = 0$. Then, the function $F(\rho)$ has a unique root $\rho = \rho_0$. Therefore, we obtain

$$U = (p_0, 0, \rho_0, a).$$

Consider the case $u_0 \neq 0$. We have

$$F'(\rho) = -\frac{2\gamma(\gamma + 1)\kappa(S_0)}{\gamma - 1}\rho^{\gamma} + 2\left(u_0^2 + \frac{2\gamma\kappa(S_0)}{\gamma - 1}\rho_0^{\gamma-1}\right)\rho,$$

so that

$$F'(\rho) > 0, \quad \rho < \rho_{\max},$$
$$F'(\rho) < 0, \quad \rho > \rho_{\max},$$

where

$$\rho_{\max} := \left(\frac{\gamma - 1}{\gamma(\gamma+1)\kappa(S_0)} u_0^2 + \frac{2}{\gamma+1} \rho_0^{\gamma-1} \right)^{\frac{1}{\gamma-1}}.$$

Moreover,

$$F(0) = F(\overline{\rho}) = -\left(\frac{a\rho_0 u_0}{a} \right)^2 < 0.$$

Thus, $F(\rho)$ admits a zero if and only if

$$F(\rho_{\max}) \geq 0,$$

or, equivalently

$$a \geq a_{\min} = a_{\min}(U_0, a_0),$$

where

$$a_{\min}(U_0, a_0) := \frac{a_0 \rho_0 |u_0|}{\sqrt{\gamma \kappa(S_0)(\rho_{\max})^{\gamma+1}}}.$$

If $a > a_{\min}$, the function $F(\rho)$ has exactly two roots denoted by $\varphi_1(U_0, a)$ and $\varphi_2(U_0, a)$, which satisfy

$$\varphi_1(U_0, a) < \rho_{\max} < \varphi_2(U_0, a).$$

The following lemma provides us with the existence of the above stationary waves.

Lemma 2.2 ([32, Lemma 3.1]) *Given $U_0 = (p_0, u_0, \rho_0, a_0)$ and $a \neq a_0$ such that $u_0 \neq 0$. There exists a stationary wave connecting U_0 to some state U if and only if $a \geq a_{\min}$. More precisely, we have the following:*
(i) *If $a < a_{\min}$, $F(\rho)$ has no roots; so there are no stationary waves.*
(ii) *If $a = a_{\min}$, $F(\rho)$ has only one root $\rho = \rho_{\max}$; so there is exactly one stationary wave connecting U_0 to $U_{\max}$, where*

$$U_{\max} := \left(\kappa(S_0)(\rho_{\max})^{\gamma}, \frac{a_0 \rho_0 u_0}{a \rho_{\max}}, \rho_{\max}, a \right).$$

(iii) *If $a > a_{\min}$, $F(\rho)$ has two distinct roots; so there are exactly two stationary waves connecting U_0 to the state U_0^s or the state U_0^b, where*

$$U_0^s := \left(\kappa(S_0)(\varphi_1(U_0, a))^{\gamma}, \frac{a_0 \rho_0 u_0}{a \varphi_1(U_0, a)}, \varphi_1(U_0, a), a \right),$$
$$U_0^b := \left(\kappa(S_0)(\varphi_2(U_0, a))^{\gamma}, \frac{a_0 \rho_0 u_0}{a \varphi_2(U_0, a)}, \varphi_2(U_0, a), a \right). \tag{2.32}$$

Using notations as Lemma 2.2, we have the following lemma.

Lemma 2.3 *Given $U_0 = (p_0, u_0, \rho_0, a_0)$ and a.*

(i) *It holds that*

$$\rho_{\max} < \rho_0, \quad U_0 \in G_2^+ \cup G_2^-,$$
$$\rho_{\max} > \rho_0, \quad U_0 \in G_1^+ \cup G_1^-.$$

(ii) *It holds that*

$$U_0^s \in G_1^+, \quad U_0^b \in G_2^+ \quad \textit{for} \quad u_0 > 0,$$
$$U_0^s \in G_1^-, \quad U_0^b \in G_2^- \quad \textit{for} \quad u_0 < 0.$$

(iii) *It holds that*

$$a_{\min} < a_0, \quad U_0 \in G_i^{\pm}, \quad i = 1, 2$$
$$a_{\min} = a_0, \quad U_0 \in \mathcal{C}^{\pm},$$
$$a_{\min} = 0, \quad u_0 = 0.$$

(iv) *If $a > a_0$, then*

$$\varphi_1(U_0, a) < \rho_0 < \varphi_2(U_0, a).$$

(v) *If $a_{\min} < a < a_0$, then*

$$\rho_0 < \varphi_1(U_0, a) < \varphi_2(U_0, a), \quad \textit{for} \quad U_0 \in G_1^{\pm},$$
$$\rho_0 > \varphi_2(U_0, a) > \varphi_1(U_0, a), \quad \textit{for} \quad U_0 \in G_2^{\pm}.$$

It follows from Lemma 2.2 that there may be two possible stationary waves from a given state U_0 to a state with a new level cross section a. Thus, it is necessary to impose some condition to select a unique physical stationary as follows.

(MC) Any stationary jump must not cross the sonic curve in the (p, u)-plane.

Observe that the admissibility criterion (MC) implies that:

- If $a > a_{\min}$ and $U_0 \in G_1^{\pm}$, then U_0^s is selected.
- If $a > a_{\min}$ and $U_0 \in G_2^{\pm}$, then U_0^b is selected.

3 The Riemann Problem Revisited

In this section, the Riemann problem for (1.1) is revisited (see [32]). We distinguish between four cases

- Case A: $U_L \in G_1^+ \cup \mathcal{C}^+$ and $a_R > a_L$;
- Case B: $U_L \in G_2^+$ and $a_R > a_L$;
- Case C: $U_R \in G_1^- \cup \mathcal{C}^-$ and $a_L > a_R$;
- Case D: $U_R \in G_2^-$ and $a_L > a_R$.

Notations (i) $W_k(U_i, U_j)$ ($S_k(U_i, U_j)$, $R_k(U_i, U_j)$) denotes the kth-wave (kth-shock, kth-rarefaction wave, respectively) connecting the left-hand state U_i to the right-hand state U_j, $k = 0, 1, 2, 3$;
(ii) $W_m(U_i, U_j) \oplus W_n(U_j, U_k)$ indicates that there is an mth-wave from the left-hand state U_i to the right-hand state U_j, followed by an nth-wave from the left-hand state U_j to the right-hand state U_k, $m, n \in \{1, 2, 3, 4\}$.
(iii) $U_0^{\#}$ denotes the state such that $\sigma_1(U_0, U_0^{\#}) = 0$. $U_0^{@}$ denotes the state such that $\sigma_3(U_0^{@}, U_0) = 0$ (see Lemma 2.1).
(iv) U_0^s, U_0^b denote the states resulting from stationary waves from U_0 (see Lemma 2.2).

3.1 Case A: $U_L \in G_1^+ \cup \mathcal{C}^+$ and $a_R > a_L$

3.1.1 Construction A1

The first part of the Riemann solution can be the stationary wave

$$W_0(U_L, U_L^s),$$

i.e.,

$$U_{\text{Rie}}(x/t; U_L, U_R) = \begin{cases} U_L = (p_L, u_L, \rho_L, a_L) & \text{if } x/t < 0, \\ U_L^s = \left(p_L^s, u_L^s, \rho_L^s, a_R\right) & \text{if } 0 < x/t < \ldots, \\ \ldots, \end{cases}$$

where

$$\rho_L^s := \varphi_1(U_L, a_R), \quad u_L^s := \frac{a_L \rho_L u_L}{a_R \rho_L^s}, \quad p_L^s := \kappa(S_L)(\rho_L^s)^\gamma.$$

If we take any $U \in \mathcal{R}_1(U_L^s)$, then the second part of the Riemann solution can be a 1-rarefaction wave

$$R_1(U_L^s, U),$$

i.e.,

$$U_{\text{Rie}}(x/t; U_L, U_R) = \begin{cases} U_L & \text{if } x/t < 0, \\ U_L^s & \text{if } 0 < x/t < \lambda_1(U_L^s), \\ \text{Fan}_1(x/t; U_L^s, U) & \text{if } \lambda_1(U_L^s) \le x/t \le \lambda_1(U), \\ U & \text{if } \lambda_1(U) < x/t < \ldots, \\ \ldots \end{cases}$$

On the other hand, if we take $U \in \mathcal{S}_1(U_L^s)$ such that $\sigma_1(U_L^s, U) > 0$ (i.e., U is located above $U_L^{s\#}$, see Lemma 2.1), then the second part of the Riemann solution can be a 1-shock wave

$$S_1(U_L^s, U),$$

i.e.,

$$U_{\text{Rie}}(x/t; U_L, U_R) = \begin{cases} U_L & \text{if } x/t < 0, \\ U_L^s & \text{if } 0 < x/t < \sigma_1(U_L^s, U), \\ U & \text{if } \sigma_1(U_L^s, U) < x/t < \ldots, \\ \ldots \end{cases}$$

Thus, if $U = (p, u, \rho, a_R) \in \mathcal{W}_1(U_L^s)$ such that U is located above $U_L^{s\#}$, then the first two parts of the Riemann solution are

$$W_0(U_L, U_L^s) \oplus W_1(U_L^s, U).$$

Therefore, we call the set

$$\{U \in \mathcal{W}_1(U_L^s): \quad U \text{ is located above } U_L^{s\#}\}$$

as *the composite wave curve* $W_0.W_1(U_L, a_R)$. Obviously, $W_0.W_1(U_L, a_R)$ is a part of the wave curve $\mathcal{W}_1(U_L^s)$ (see Fig. 2). If we have an intersection in the (p, u)-plane

$$(p, u) = \mathcal{W}_3^B(U_R) \cap W_0.W_1(U_L, a_R),$$

then the Riemann problem for (1.1) has a solution of the form

$$W_0(U_L, U_L^s) \oplus W_1(U_L^s, U) \oplus W_2(U, U^*) \oplus W_3(U^*, U_R), \tag{3.1}$$

where

$$U^* = (p, u, \rho^*, a_R) \in \mathcal{W}_3(U_R).$$

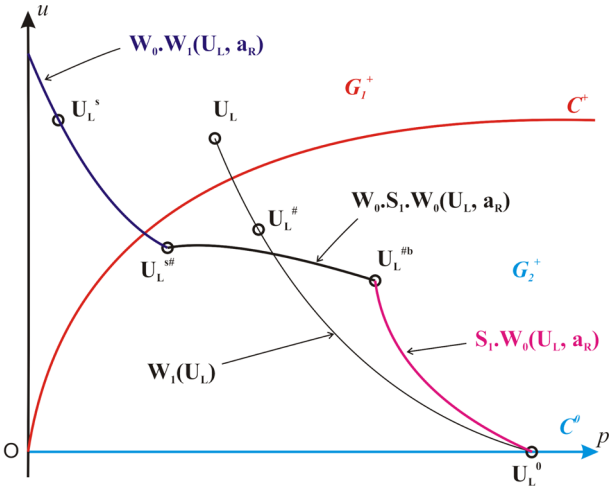

Fig. 2 The composite wave curves: $W_0.W_1(U_L, a_R)$, $W_0.S_1.W_0(U_L, a_R)$, and $S_1.W_0(U_L, a_R)$ in the (p, u)-plane

Explicitly, the form (3.1) can be seen as follows.

- If $U \in \mathcal{R}_1(U_L^s)$ and $U^* \in \mathcal{R}_3^B(U_R)$, then the form (3.1) yields

$$U_{\text{Rie}}(x/t; U_L, U_R) = \begin{cases} U_L & \text{if } x/t < 0, \\ U_L^s & \text{if } 0 < x/t < \lambda_1(U_L^s), \\ \text{Fan}_1(x/t; U_L^s, U) & \text{if } \lambda_1(U_L^s) \le x/t \le \lambda_1(U), \\ U & \text{if } \lambda_1(U) < x/t < \lambda_2(U) = \lambda_2(U^*), \\ U^* & \text{if } \lambda_2(U^*) < x/t < \lambda_3(U^*), \\ \text{Fan}_3(x/t; U^*, U_R) & \text{if } \lambda_3(U^*) \le x/t \le \lambda_3(U_R), \\ U_R & \text{if } x/t > \lambda_3(U_R). \end{cases}$$

- If $U \in \mathcal{R}_1(U_L^s)$ and $U^* \in \mathcal{S}_3^B(U_R)$, then the form (3.1) yields

$$U_{\text{Rie}}(x/t; U_L, U_R) = \begin{cases} U_L & \text{if } x/t < 0, \\ U_L^s & \text{if } 0 < x/t < \lambda_1(U_L^s), \\ \text{Fan}_1(x/t; U_L^s, U) & \text{if } \lambda_1(U_L^s) \le x/t \le \lambda_1(U), \\ U & \text{if } \lambda_1(U) < x/t < \lambda_2(U) = \lambda_2(U^*), \\ U^* & \text{if } \lambda_2(U^*) < x/t < \sigma_3(U^*, U_R), \\ U_R & \text{if } x/t > \sigma_3(U^*, U_R). \end{cases}$$

- If $U \in \mathcal{S}_1(U_L^s)$ and $U^* \in \mathcal{R}_3^B(U_R)$, then the form (3.1) yields

$$U_{\text{Rie}}(x/t; U_L, U_R) = \begin{cases} U_L & \text{if } x/t < 0, \\ U_L^s & \text{if } 0 < x/t < \sigma_1(U_L^s, U), \\ U, & \text{if } \sigma_1(U_L^s, U) < x/t < \lambda_2(U) = \lambda_2(U^*), \\ U^* & \text{if } \lambda_2(U^*) < x/t < \lambda_3(U^*), \\ \text{Fan}_3(x/t; U^*, U_R) & \text{if } \lambda_3(U^*) \le x/t \le \lambda_3(U_R), \\ U_R & \text{if } x/t > \lambda_3(U_R). \end{cases}$$

- If $U \in \mathcal{S}_1(U_L^s)$ and $U^* \in \mathcal{S}_3^B(U_R)$, then the form (3.1) yields

$$U_{\text{Rie}}(x/t; U_L, U_R) = \begin{cases} U_L & \text{if } x/t < 0, \\ U_L^s & \text{if } 0 < x/t < \sigma_1(U_L^s, U), \\ U & \text{if } \sigma_1(U_L^s, U) < x/t < \lambda_2(U) = \lambda_2(U^*), \\ U^* & \text{if } \lambda_2(U^*) < x/t < \sigma_3(U^*, U_R), \\ U_R & \text{if } x/t > \sigma_3(U^*, U_R). \end{cases}$$

Algorithm to Compute the Intersection Point $(p, u) = \mathcal{W}_3^B(U_R) \cap W_0.W_1(U_L, a_R)$. Assume that $U_L^{s\#}$ is located below the curve $\mathcal{W}_3^B(U_R)$ in the $(p, u)-$plane.

Step 1 Set $p_1 = 0$, $p_2 = p_L^{s\#}$;

Step 2 Compute $p = \dfrac{p_1 + p_2}{2}$; Compute u such that $(p, u) \in \mathcal{W}_1(U_L^s)$ in the (p, u)-plane;

Step 3 – If (p, u) belongs to $\mathcal{W}_3^B(U_R)$ in the $(p, u)-$plane, end;
– If (p, u) is located above $\mathcal{W}_3^B(U_R)$ in the $(p, u)-$plane, set $p_1 = p$ and return Step 2;
– If (p, u) is located below $\mathcal{W}_3^B(U_R)$ in the $(p, u)-$plane, set $p_2 = p$ and return Step 2.

3.1.2 Construction A2

Fix a cross section level a_M between a_L and a_R. The first part of the Riemann solution can be a stationary wave

$$W_0(U_L, U_L^s),$$

where

$$\begin{aligned} &U_L^s = \left(p_L^s, u_L^s, \rho_L^s, a_M\right), \\ &\rho_L^s := \varphi_1(U_L, a_M), \quad u_L^s := \frac{a_L \rho_L u_L}{a_M \rho_L^s}, \quad p_L^s := \kappa(S_L)(\rho_L^s)^\gamma. \end{aligned} \tag{3.2}$$

The second part of the Riemann solution is a 1-shock wave with zero speed

$$S_1(U_L^s, U_L^{s\#}).$$

The third part is again a stationary wave

$$W_0(U_L^{s\#}, U_L^{s\#b}),$$

where

$$\begin{aligned} &U_L^{s\#b} = (p, u, \rho, a_R), \\ &\rho := \varphi_2(U_L^{s\#}, a_R), \quad u := \frac{a_M \rho_L^{s\#} u_L^{s\#}}{a_R \rho}, \quad p := \kappa(S_L^{s\#})\rho^\gamma. \end{aligned} \tag{3.3}$$

Because these three parts are discontinuity waves with same zero speed, we have a wave collision (resonant case), i.e., $W_0(U_L, U_L^s) \oplus S_1(U_L^s, U_L^{s\#}) \oplus W_0(U_L^{s\#}, U_L^{s\#b})$ is just a discontinuity wave with zero speed

$$U_{\text{Rie}}(x/t; U_L, U_R) = \begin{cases} U_L & \text{if } x/t < 0, \\ U_L^{s\#b} & \text{if } 0 < x/t < \ldots, \\ \ldots \end{cases}$$

We call the set

$$\{U_L^{s\#b} : \quad a_M \text{ varies between } a_L \text{ and } a_R\}$$

as *the composite wave curve* $W_0.S_1.W_0(U_L, a_R)$. It is not difficult to check that $U_L^{\#b}$ and $U_L^{s\#}$ are two end-points of $W_0.S_1.W_0(U_L, a_R)$ (see Fig. 2). Therefore, if we have an intersection in the (p, u)-plane

$$(p, u) = \mathcal{W}_3^B(U_R) \cap W_0.S_1.W_0(U_L, a_R),$$

then the Riemann problem for (1.1) has a solution of the form

$$W_0(U_L, U_L^s) \oplus S_1(U_L^s, U_L^{s\#}) \oplus W_0(U_L^{s\#}, U_L^{s\#b}) \oplus W_2(U_L^{s\#b}, U^*) \oplus W_3(U^*, U_R), \quad (3.4)$$

where

$$U^* = (p, u, \rho^*, a_R) \in \mathcal{W}_3(U_R).$$

Explicitly, the form (3.4) can be seen as follows.

- If $U^* \in \mathcal{R}_3^B(U_R)$, then the form (3.4) yields

$$U_{\text{Rie}}(x/t; U_L, U_R) = \begin{cases} U_L & \text{if } x/t < 0, \\ U_L^{s\#b} & \text{if } 0 < x/t < \lambda_2(U_L^{s\#b}) = \lambda_2(U^*), \\ U^* & \text{if } \lambda_2(U^*) < x/t < \lambda_3(U^*), \\ \text{Fan}_3(x/t; U^*, U_R) & \text{if } \lambda_3(U^*) \le x/t \le \lambda_3(U_R), \\ U_R & \text{if } x/t > \lambda_3(U_R). \end{cases}$$

- If $U^* \in \mathcal{S}_3^B(U_R)$, then the form (3.4) yields

$$U_{\text{Rie}}(x/t; U_L, U_R) = \begin{cases} U_L & \text{if } x/t < 0, \\ U_L^{s\#b} & \text{if } 0 < x/t < \lambda_2(U_L^{s\#b}) = \lambda_2(U^*), \\ U^* & \text{if } \lambda_2(U^*) < x/t < \sigma_3(U^*, U_R), \\ U_R & \text{if } x/t > \sigma_3(U^*, U_R). \end{cases}$$

Algorithm to Compute the Intersection Point $(p, u) = \mathcal{W}_3^B(U_R) \cap W_0.S_1.W_0\ (U_L, a_R)$. Assume that $U_L^{s\#}$ is located above $\mathcal{W}_3^B(U_R)$ and $U_L^{\#b}$ is located below $\mathcal{W}_3^B(U_R)$ in the (p, u)-plane.

Step 1 Set $a_1 = a_L, a_2 = a_R$;

Step 2 Compute $a_M = \frac{a_1+a_2}{2}$; Compute U_L^s as in (3.2); Compute $U_L^{s\#}$; Compute $U_L^{s\#b} = (p, u, \rho, a_R)$ as in (3.3);

Step 3 • If (p, u) belongs to $\mathcal{W}_3^B(U_R)$ in the (p, u)-plane, end;

- If (p, u) is located above $\mathcal{W}_3^B(U_R)$ in the (p, u)-plane, set $a_2 = a_M$ and return Step 2;
- If (p, u) is located below $\mathcal{W}_3^B(U_R)$ in the (p, u)-plane, set $a_1 = a_M$ and return Step 2.

3.1.3 Construction A3

Take any state $U = (p, u, \rho, a_L) \in \mathcal{S}_1(U_L) \cap G_2^+$ such that $\sigma_1(U_L, U) < 0$, i.e., U is located between $U_L^\#$ and U_L^0, where

$$U_L^0 = (p_L^0, u_L^0, \rho_L^0, a_L) = \mathcal{W}_1(U_L) \cap \mathcal{C}^0.$$

Then, the first part of the Riemann solution can be a 1-shock wave with negative speed

$$S_1(U_L, U).$$

Next, the second part of the Riemann solution can be a stationary wave

$$W_0(U, U^b),$$

where

$$U^b = \left(p^b, u^b, \rho^b, a_R\right),$$
$$\rho^b := \varphi_2(U, a_R), \quad u^b := \frac{a_L \rho u}{a_R \rho^b}, \quad p^b := \kappa(S)(\rho^b)^\gamma. \tag{3.5}$$

The set

$$\{U^b : \quad U \text{ is located between } U_L^{\#} \text{ and } U_L^0 \text{ on } \mathcal{S}_1(U_L)\}$$

is called the composite wave curve $S_1.W_0(U_L, a_R)$. Obviously, $U_L^{\#b}$ and U_L^0 are two endpoints of $S_1.W_0(U_L, a_R)$ (see Fig. 2). Therefore, if we have an intersection in the (p, u)-plane

$$(p^b, u^b) = \mathcal{W}_3^B(U_R) \cap S_1.W_0(U_L, a_R),$$

then the Riemann problem for (1.1) has a solution of the form

$$S_1(U_L, U) \oplus W_0(U, U^b) \oplus W_2(U^b, U^*) \oplus W_3(U^*, U_R), \tag{3.6}$$

where

$$U^* = (p^b, u^b, \rho^*, a_R) \in \mathcal{W}_3^B(U_R).$$

Explicitly, the form (3.6) can be seen as follows.
• $U^* \in \mathcal{R}_3^B(U_R)$, then the form (3.6) yields

$$U_{\text{Rie}}(x/t; U_L, U_R) = \begin{cases} U_L & \text{if } x/t < \sigma_1(U_L, U), \\ U & \text{if } \sigma_1(U_L, U) < x/t < 0, \\ U^b & \text{if } 0 < x/t < \lambda_2(U^b) = \lambda_2(U^*), \\ U^* & \text{if } \lambda_2(U^*) < x/t < \lambda_3(U^*), \\ \text{Fan}_3(x/t; U^*, U_R) & \text{if } \lambda_3(U^*) \le x/t \le \lambda_3(U_R), \\ U_R & \text{if } x/t > \lambda_3(U_R). \end{cases}$$

• $U^* \in \mathcal{S}_3^B(U_R)$, then the form (3.6) yields

$$U_{\text{Rie}}(x/t; U_L, U_R) = \begin{cases} U_L & \text{if } x/t < \sigma_1(U_L, U), \\ U & \text{if } \sigma_1(U_L, U) < x/t < 0, \\ U^b & \text{if } 0 < x/t < \lambda_2(U^b) = \lambda_2(U^*), \\ U^* & \text{if } \lambda_2(U^*) < x/t < \sigma_3(U^*, U_R), \\ U_R & \text{if } x/t > \sigma_3(U^*, U_R). \end{cases}$$

Algorithm to Compute the State U and the Intersection Point $(p^b, u^b) = \mathcal{W}_3^B(U_R) \cap S_1.W_0(U_L, a_R)$. Assume that $U_L^{\#b}$ is located above $\mathcal{W}_3^B(U_R)$ and U_L^0 is located below $\mathcal{W}_3^B(U_R)$ in the (p, u)-plane.

Step 1 Set $p_1 = p_L^{\#}$, $p_2 = p_L^0$;

Step 2 Compute $p = \frac{p_1 + p_2}{2}$; Compute $U = (p, u, \rho, a_L) \in \mathcal{S}_1(U_L)$; Compute $U^b = (p^b, u^b, \rho^b, a_R)$ as in (3.5);

Step 3 – If (p^b, u^b) belongs to $\mathcal{W}_3^B(U_R)$ in the (p, u)-plane, end;
– If (p^b, u^b) is located above $\mathcal{W}_3^B(U_R)$ in the (p, u)-plane, set $p_1 = p$ and return Step 2;
– If (p^b, u^b) is located below $\mathcal{W}_3^B(U_R)$ in the (p, u)-plane, set $p_2 = p$ and return Step 2.

3.2 Case B: $U_L \in G_2^+$ and $a_R > a_L$

3.2.1 Construction B1

The first part of the Riemann solution can be the 1-rarefaction wave

$$R_1(U_L, U_L^+),$$

where

$$U_L^+ = (p_L^+, u_L^+, \rho_L^+, a_L) = \mathcal{W}_1(U_L) \cap \mathcal{C}^+.$$

The second part of the Riemann solution can be the stationary wave

$$W_0(U_L^+, U_L^{+s}),$$

where

$$U_L^{+s} = \left(p_L^{+s}, u_L^{+s}, \rho_L^{+s}, a_R\right),$$

$$\rho_L^{+s} := \varphi_1(U_L^+, a_R), \quad u_L^{+s} := \frac{a_L \rho_L^+ u_L^+}{a_R \rho_L^{+s}}, \quad p_L^{+s} := \kappa(S_L)(\rho_L^{+s})^\gamma.$$

Take any state $U = (p, u, \rho, a_R) \in \mathcal{W}_1(U_L^{+s})$ such that U is located above $U_L^{+s\#}$. Then, the third part of the Riemann solution can be a 1-wave

$$W_1(U_L^{+s}, U).$$

We call the set

$$\{U \in \mathcal{W}_1(U_L^{+s}) : \quad U \text{ is located above } U_L^{+s\#}\}$$

as the composite wave curve $R_1.W_0.W_1(U_L, a_R)$ (see Fig. 3). If we have an intersection in the $(p, u)-$plane

$$(p, u) = \mathcal{W}_3^B(U_R) \cap R_1.W_0.W_1(U_L, a_R),$$

then the Riemann problem for (1.1) has a solution of the form

$$R_1(U_L, U_L^+) \oplus W_0(U_L^+, U_L^{+s}) \oplus W_1(U_L^{+s}, U) \oplus W_2(U, U^*) \oplus W_3(U^*, U_R), \tag{3.7}$$

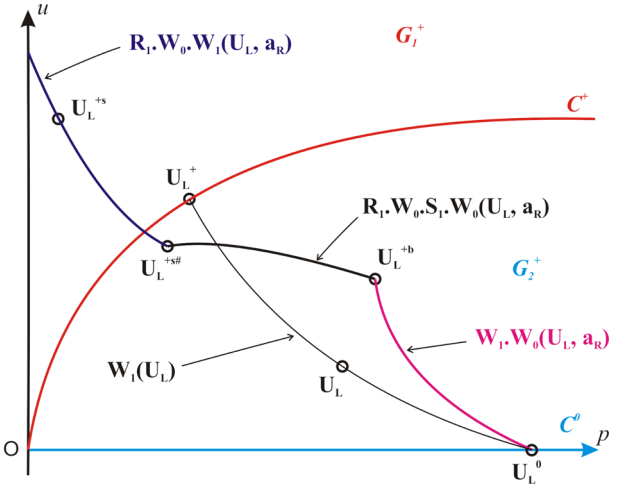

Fig. 3 The composite wave curves: $R_1.W_0.W_1(U_L, a_R)$, $R_1.W_0.S_1.W_0(U_L, a_R)$ and $W_1.W_0(U_L, a_R)$ in the (p, u)-plane

where

$$U^* = (p, u, \rho^*, a_R) \in \mathcal{W}_3^B(U_R).$$

Explicitly, the form (3.7) can be seen as follows.

• If $U \in \mathcal{R}_1(U_L^{+s})$ and $U^* \in \mathcal{R}_3^B(U_R)$, then the form (3.7) yields

$$U_{\text{Rie}}(x/t; U_L, U_R) = \begin{cases} U_L & \text{if } x/t < \lambda_1(U_L), \\ \text{Fan}_1(x/t; U_L, U_L^+) & \text{if } \lambda_1(U_L) \le x/t \le \lambda_1(U_L^+) = 0, \\ U_L^{+s} & \text{if } 0 < x/t < \lambda_1(U_L^{+s}), \\ \text{Fan}_1(x/t; U_L^{+s}, U) & \text{if } \lambda_1(U_L^{+s}) \le x/t \le \lambda_1(U), \\ U & \text{if } \lambda_1(U) < x/t < \lambda_2(U) = \lambda_2(U^*), \\ U^* & \text{if } \lambda_2(U^*) < x/t < \lambda_3(U^*), \\ \text{Fan}_3(x/t; U^*, U_R) & \text{if } \lambda_3(U^*) \le x/t \le \lambda_3(U_R), \\ U_R & \text{if } x/t > \lambda_3(U_R). \end{cases}$$

• If $U \in \mathcal{R}_1(U_L^{+s})$ and $U^* \in \mathcal{S}_3^B(U_R)$, then the form (3.7) yields

$$U_{\text{Rie}}(x/t; U_L, U_R) = \begin{cases} U_L & \text{if } x/t < \lambda_1(U_L), \\ \text{Fan}_1(x/t; U_L, U_L^+) & \text{if } \lambda_1(U_L) \le x/t \le \lambda_1(U_L^+) = 0, \\ U_L^{+s} & \text{if } 0 < x/t < \lambda_1(U_L^{+s}), \\ \text{Fan}_1(x/t; U_L^{+s}, U) & \text{if } \lambda_1(U_L^{+s}) \le x/t \le \lambda_1(U), \\ U & \text{if } \lambda_1(U) < x/t < \lambda_2(U) = \lambda_2(U^*), \\ U^* & \text{if } \lambda_2(U^*) < x/t < \sigma_3(U^*, U_R), \\ U_R & \text{if } x/t > \sigma_3(U^*, U_R). \end{cases}$$

• If $U \in \mathcal{S}_1(U_L^{+s})$ and $U^* \in \mathcal{R}_3^B(U_R)$, then the form (3.7) yields

$$U_{\text{Rie}}(x/t; U_L, U_R) = \begin{cases} U_L & \text{if } x/t < \lambda_1(U_L), \\ \text{Fan}_1(x/t; U_L, U_L^+) & \text{if } \lambda_1(U_L) \le x/t \le \lambda_1(U_L^+) = 0, \\ U_L^{+s} & \text{if } 0 < x/t < \sigma_1(U_L^{+s}, U), \\ U & \text{if } \sigma_1(U_L^{+s}, U) < x/t < \lambda_2(U) = \lambda_2(U^*), \\ U^* & \text{if } \lambda_2(U^*) < x/t < \lambda_3(U^*), \\ \text{Fan}_3(x/t; U^*, U_R) & \text{if } \lambda_3(U^*) \le x/t \le \lambda_3(U_R), \\ U_R & \text{if } x/t > \lambda_3(U_R). \end{cases}$$

• If $U \in \mathcal{S}_1(U_L^{+s})$ and $U^* \in \mathcal{S}_3^B(U_R)$, then the form (3.7) yields

$$U_{\text{Rie}}(x/t; U_L, U_R) = \begin{cases} U_L & \text{if } x/t < \lambda_1(U_L), \\ \text{Fan}_1(x/t; U_L, U_L^+) & \text{if } \lambda_1(U_L) \le x/t \le \lambda_1(U_L^+) = 0, \\ U_L^{+s} & \text{if } 0 < x/t < \sigma_1(U_L^{+s}, U), \\ U & \text{if } \sigma_1(U_L^{+s}, U) < x/t < \lambda_2(U) = \lambda_2(U^*), \\ U^* & \text{if } \lambda_2(U^*) < x/t < \sigma_3(U^*, U_R), \\ U_R & \text{if } x/t > \sigma_3(U^*, U_R). \end{cases}$$

Algorithm to Compute the Intersection Point $(p, u) = \mathcal{W}_3^B(U_R) \cap R_1.W_0.W_1\ (U_L, a_R)$. Similar to case A, since $R_1.W_0.W_1(U_L, a_R) \equiv W_0.W_1(U_L^+, a_R)$.

3.2.2 Construction B2

The first part of the Riemann solution can be the 1-rarefaction wave

$$R_1(U_L, U_L^+),$$

where

$$U_L^+ = (p_L^+, u_L^+, \rho_L^+, a_L) = \mathcal{W}_1(U_L) \cap \mathcal{C}^+.$$

Fix a cross section a_M between a_L and a_R. The second part of the Riemann solution can be a stationary wave

$$W_0(U_L^+, U_L^{+s}),$$

where

$$U_L^{+s} = \left(p_L^{+s}, u_L^{+s}, \rho_L^{+s}, a_M\right),$$
$$\rho_L^{+s} := \varphi_1(U_L^+, a_M), \quad u_L^{+s} := \frac{a_L \rho_L^+ u_L^+}{a_M \rho_L^{+s}}, \quad p_L^{+s} := \kappa(S_L)(\rho_L^{+s})^\gamma.$$

The third part of the Riemann solution can be a 1-shock wave with zero speed

$$S_1(U_L^{+s}, U_L^{+s\#}).$$

The fourth part of the Riemann solution can be again a stationary wave

$$W_0(U_L^{+s\#}, U_L^{+s\#b}),$$

where

$$U_L^{+s\#b} = (p, u, \rho, a_R),$$
$$\rho := \varphi_2(U_L^{+s\#}, a_R), \quad u := \frac{a_M \rho_L^{+s\#} u_L^{+s\#}}{a_R \rho}, \quad p := \kappa(S_L^{+s\#})\rho^\gamma.$$

We call the set

$$\{U_L^{+s\#b} : \quad a_M \text{ varies between } a_L \text{ and } a_R\}$$

as the composite wave curve $R_1.W_0.S_1.W_0(U_L, a_R)$. It is not difficult to check that $U_L^{+s\#}$ and U_L^{+b} are two end-points of $R_1.W_0.S_1.W_0(U_L, a_R)$ (see Fig. 3). Therefore, if we have an intersection in the $(p, u)-$plane

$$(p, u) = \mathcal{W}_3^B(U_R) \cap R_1.W_0.S_1.W_0(U_L, a_R),$$

then the Riemann problem for (1.1) has a solution of the form

$$R_1(U_L, U_L^+) \oplus W_0(U_L^+, U_L^{+s}) \oplus S_1(U_L^{+s}, U_L^{+s\#}) \oplus W_0(U_L^{+s\#}, U_L^{+s\#b}) \oplus W_2(U, U^*) \oplus W_3(U^*, U_R), \tag{3.8}$$

where

$$U^* = (p, u, \rho^*, a_R) \in \mathcal{W}_3^B(U_R).$$

Explicitly, the form (3.8) can be seen as follows.
• If $U^* \in \mathcal{R}_3^B(U_R)$, then the form (3.8) yields

$$U_{\text{Rie}}(x/t; U_L, U_R) = \begin{cases} U_L & \text{if } x/t < \lambda_1(U_L), \\ \text{Fan}_1(x/t; U_L, U_L^+) & \text{if } \lambda_1(U_L) \le x/t \le \lambda_1(U_L^+) = 0, \\ U_L^{+s\#b} & \text{if } 0 < x/t < \lambda_2(U_L^{+s\#b}) = \lambda_2(U^*), \\ U^* & \text{if } \lambda_2(U^*) < x/t < \lambda_3(U^*), \\ \text{Fan}_3(x/t; U^*, U_R) & \text{if } \lambda_3(U^*) \le x/t \le \lambda_3(U_R), \\ U_R & \text{if } x/t > \lambda_3(U_R). \end{cases}$$

• If $U^* \in \mathcal{S}_3^B(U_R)$, then the form (3.8) yields

$$U_{\text{Rie}}(x/t; U_L, U_R) = \begin{cases} U_L & \text{if } x/t < \lambda_1(U_L), \\ \text{Fan}_1(x/t; U_L, U_L^+) & \text{if } \lambda_1(U_L) \le x/t \le \lambda_1(U_L^+) = 0, \\ U_L^{+s\#b} & \text{if } 0 < x/t < \lambda_2(U_L^{+s\#b}) = \lambda_2(U^*), \\ U^* & \text{if } \lambda_2(U^*) < x/t < \sigma_3(U^*, U_R), \\ U_R & \text{if } x/t > \sigma_3(U^*, U_R). \end{cases}$$

Algorithm to Compute the Intersection Point $(p, u) = \mathcal{W}_3^B(U_R) \cap R_1.W_0.S_1.W_0(U_L, a_R)$. Similar to case A, since $R_1.W_0.S_1.W_0(U_L, a_R) \equiv W_0.S_1.W_0(U_L^+, a_R)$.

3.2.3 Construction B3

Take a state $U = (p, u, \rho, a_L) \in \mathcal{W}_1(U_L)$ such that $U \in G_2^+$, i.e., U is located between U_L^+ and U_L^0, where

$$U_L^+ = (p_L^+, u_L^+, \rho_L^+, a_L) = \mathcal{W}_1(U_L) \cap \mathcal{C}^+,$$
$$U_L^0 = (p_L^0, u_L^0, \rho_L^0, a_L) = \mathcal{W}_1(U_L) \cap \mathcal{C}^0.$$

Then, the first part of the Riemann solution can be a 1-wave

$$W_1(U_L, U).$$

Next, the second part of the Riemann solution can be a stationary wave

$$W_0(U, U^b),$$

where

$$U^b = \left(p^b, u^b, \rho^b, a_R\right),$$
$$\rho^b := \varphi_2(U, a_R), \quad u^b := \frac{a_L \rho u}{a_R \rho^b}, \quad p^b := \kappa(S)(\rho^b)^\gamma.$$

We call the set

$$\{U^b : \quad U \text{ is located between } U_L^+ \text{ and } U_L^0 \text{ on } \mathcal{W}_1(U_L)\}$$

as the composite wave curve $W_1.W_0(U_L, a_R)$. Obviously, U_L^{+b} and U_L^0 are two end-points of $W_1.W_0(U_L, a_R)$ (see Fig. 3). Therefore, if we have an intersection in the $(p, u)-$plane

$$(p^b, u^b) = \mathcal{W}_3^B(U_R) \cap W_1.W_0(U_L, a_R),$$

then the Riemann problem for (1.1) has a solution of the form

$$W_1(U_L, U) \oplus W_0(U, U^b) \oplus W_2(U^b, U^*) \oplus W_3(U^*, U_R), \tag{3.9}$$

where

$$U^* = (p^b, u^b, \rho^*, a_R) \in \mathcal{W}_3^B(U_R).$$

Explicitly, the form (3.9) can be seen as follows.

• If $U \in \mathcal{R}_1(U_L)$ and $U^* \in \mathcal{R}_3^B(U_R)$, then the form (3.9) yields

$$U_{\text{Rie}}(x/t; U_L, U_R) = \begin{cases} U_L & \text{if } x/t < \lambda_1(U_L), \\ \text{Fan}_1(x/t; U_L, U) & \text{if } \lambda_1(U_L) \le x/t \le \lambda_1(U), \\ U & \text{if } \lambda_1(U) < x/t < 0, \\ U^b & \text{if } 0 < x/t < \lambda_2(U^b) = \lambda_2(U^*), \\ U^* & \text{if } \lambda_2(U^*) < x/t < \lambda_3(U^*), \\ \text{Fan}_3(x/t; U^*, U_R) & \text{if } \lambda_3(U^*) \le x/t \le \lambda_3(U_R), \\ U_R & \text{if } x/t > \lambda_3(U_R). \end{cases}$$

• If $U \in \mathcal{R}_1(U_L)$ and $U^* \in \mathcal{S}_3^B(U_R)$, then the form (3.9) yields

$$U_{\text{Rie}}(x/t; U_L, U_R) = \begin{cases} U_L & \text{if } x/t < \lambda_1(U_L), \\ \text{Fan}_1(x/t; U_L, U) & \text{if } \lambda_1(U_L) \le x/t \le \lambda_1(U), \\ U & \text{if } \lambda_1(U) < x/t < 0, \\ U^b & \text{if } 0 < x/t < \lambda_2(U^b) = \lambda_2(U^*), \\ U^* & \text{if } \lambda_2(U^*) < x/t < \sigma_3(U^*, U_R), \\ U_R & \text{if } x/t > \sigma_3(U^*, U_R). \end{cases}$$

• If $U \in \mathcal{S}_1(U_L)$ and $U^* \in \mathcal{R}_3^B(U_R)$, then the form (3.9) yields

$$U_{\text{Rie}}(x/t; U_L, U_R) = \begin{cases} U_L & \text{if } x/t < \sigma_1(U_L, U), \\ U & \text{if } \sigma_1(U_L, U) < x/t < 0, \\ U^b & \text{if } 0 < x/t < \lambda_2(U^b) = \lambda_2(U^*), \\ U^* & \text{if } \lambda_2(U^*) < x/t < \lambda_3(U^*), \\ \text{Fan}_3(x/t; U^*, U_R) & \text{if } \lambda_3(U^*) \le x/t \le \lambda_3(U_R), \\ U_R & \text{if } x/t > \lambda_3(U_R). \end{cases}$$

• If $U \in \mathcal{S}_1(U_L)$ and $U^* \in \mathcal{S}_3^B(U_R)$, then the form (3.9) yields

$$U_{\text{Rie}}(x/t; U_L, U_R) = \begin{cases} U_L, & \text{if } x/t < \sigma_1(U_L, U), \\ U, & \text{if } \sigma_1(U_L, U) < x/t < 0, \\ U^b, & \text{if } 0 < x/t < \lambda_2(U^b) = \lambda_2(U^*), \\ U^*, & \text{if } \lambda_2(U^*) < x/t < \sigma_3(U^*, U_R), \\ U_R, & \text{if } x/t > \sigma_3(U^*, U_R). \end{cases}$$

Algorithm to Compute the State U and the Intersection Point $(p^b, u^b) = \mathcal{W}_3^B(U_R) \cap W_1.W_0(U_L, a_R)$. Similar to Construction A3, but the assignment $p_1 = p_L^{\#}$ in Step 1 is replaced by $p_1 = p_L^+$.

3.3 Case C: $U_R \in G_1^- \cup \mathcal{C}^-$ and $a_L > a_R$

3.3.1 Construction C1

The last part of the Riemann solution can be the stationary wave

$$W_0(U_R^s, U_R),$$

i.e.,

$$U_{\text{Rie}}(x/t; U_L, U_R) = \begin{cases} \ldots, \\ U_R^s & \text{if } \ldots < x/t < 0, \\ U_R & \text{if } x/t > 0, \end{cases}$$

where

$$U_R^s = \left(p_R^s, u_R^s, \rho_R^s, a_L\right),$$
$$\rho_R^s := \varphi_1(U_R, a_L), \quad u_R^s := \frac{a_R \rho_R u_R}{a_L \rho_R^s}, \quad p_R^s := \kappa(S_R)(\rho_R^s)^\gamma.$$

Take a state $U = (p, u, \rho, a_L) \in \mathcal{W}_3(U_R^s)$ such that U is located below $U_R^{s@}$. Then, the next part of the Riemann solution from the end can be a 3-wave

$$W_3(U, U_R^s).$$

We call the set

$$\{U \in \mathcal{W}_3^B(U_R^s): \quad U \text{ is located below } U_R^{s@}\}$$

as the backward composite wave curve $W_0^B.W_3^B(U_R, a_L)$ (see Fig. 4). If the wave curve $\mathcal{W}_1(U_L)$ intersects $W_0^B.W_3^B(U_R, a_L)$ at a point (p, u) in the (p, u)-plane, then the Riemann problem for (1.1) has a solution of the form

$$W_1(U_L, U^*) \oplus W_2(U^*, U) \oplus W_3(U, U_R^s) \oplus W_0(U_R^s, U_R), \tag{3.10}$$

where

$$U^* = (p, u, \rho^*, a_L) \in \mathcal{W}_1(U_L).$$

Explicitly, the form (3.10) can be seen as follows.
• If $U \in \mathcal{R}_3^B(U_R^s)$ and $U^* \in \mathcal{R}_1(U_L)$, then the form (3.10) yields

$$U_{\text{Rie}}(x/t; U_L, U_R) = \begin{cases} U_L & \text{if } x/t < \lambda_1(U_L), \\ \text{Fan}_1(x/t; U_L, U^*) & \text{if } \lambda_1 \le x/t \le \lambda_1(U_*), \\ U^* & \text{if } \lambda_1(U^*) < x/t < \lambda_2(U^*) = \lambda_2(U), \\ U & \text{if } \lambda_2(U) < x/t < \lambda_3(U), \\ \text{Fan}_3(x/t; U, U_R^s) & \text{if } \lambda_3(U) \le x/t \le \lambda_3(U_R^s), \\ U_R^s & \text{if } \lambda_3(U_R^s) < x/t < 0, \\ U_R & \text{if } x/t > 0. \end{cases}$$

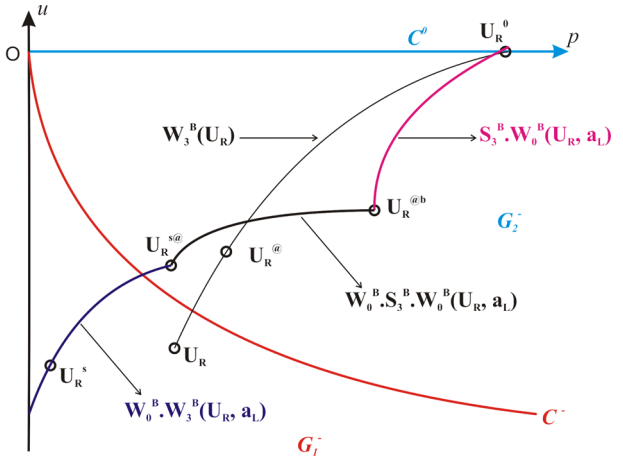

Fig. 4 The composite wave curves: $W_0^B.W_3^B(U_R, a_L)$, $W_0^B.S_3^B.W_0^B(U_R, a_L)$ and $S_3^B.W_0^B(U_R, a_L)$ in the (p, u)-plane

• If $U \in \mathcal{S}_3^B(U_R^s)$ and $U^* \in \mathcal{R}_1(U_L)$, then the form (3.10) yields

$$U_{\text{Rie}}(x/t; U_L, U_R) = \begin{cases} U_L & \text{if } x/t < \lambda_1(U_L), \\ \text{Fan}_1(x/t; U_L, U^*) & \text{if } \lambda_1 \le x/t \le \lambda_1(U_*), \\ U^* & \text{if } \lambda_1(U^*) < x/t < \lambda_2(U^*) = \lambda_2(U), \\ U & \text{if } \lambda_2(U) < x/t < \sigma_3(U, U_R^s), \\ U_R^s & \text{if } \sigma_3(U, U_R^s) < x/t < 0, \\ U_R & \text{if } x/t > 0. \end{cases}$$

• If $U \in \mathcal{R}_3^B(U_R^s)$ and $U^* \in \mathcal{S}_1(U_L)$, then the form (3.10) yields

$$U_{\text{Rie}}(x/t; U_L, U_R) = \begin{cases} U_L & \text{if } x/t < \sigma_1(U_L, U^*), \\ U^* & \text{if } \sigma_1(U_L, U^*) < x/t < \lambda_2(U^*) = \lambda_2(U), \\ U & \text{if } \lambda_2(U) < x/t < \lambda_3(U), \\ \text{Fan}_3(x/t; U, U_R^s) & \text{if } \lambda_3(U) \le x/t \le \lambda_3(U_R^s), \\ U_R^s & \text{if } \lambda_3(U_R^s) < x/t < 0, \\ U_R & \text{if } x/t > 0. \end{cases}$$

• If $U \in \mathcal{S}_3^B(U_R^s)$ and $U^* \in \mathcal{S}_1(U_L)$, then the form (3.10) yields

$$U_{\text{Rie}}(x/t; U_L, U_R) = \begin{cases} U_L & \text{if } x/t < \sigma_1(U_L, U^*), \\ U^* & \text{if } \sigma_1(U_L, U^*) < x/t < \lambda_2(U^*) = \lambda_2(U), \\ U & \text{if } \lambda_2(U) < x/t < \sigma_3(U, U_R^s), \\ U_R^s & \text{if } \sigma_3(U, U_R^s) < x/t < 0, \\ U_R & \text{if } x/t > 0. \end{cases}$$

Algorithm to Compute the Intersection Point $(p, u) = \mathcal{W}_1(U_L) \cap W_0^B.W_3^B\ (U_R, a_L)$. Assume that $U_R^{s@}$ is located above the curve $\mathcal{W}_1(U_L)$ in the $(p, u) - plane$.

Step 1 Set $p_1 = 0$, $p_2 = p_R^{s@}$;

Step 2 Compute $p = \frac{p_1+p_2}{2}$ and u such that $(p, u) \in \mathcal{W}_3^B(U_R^s)$ in the $(p, u)-$plane;

Step 3 – If (p, u) belongs to $\mathcal{W}_1(U_L)$ in the (p, u)-plane, end;
– If (p, u) is located above $\mathcal{W}_1(U_L)$ in the (p, u)-plane, set $p_2 = p$ and return Step 2;
– If (p, u) is located below $\mathcal{W}_1(U_L)$ in the (p, u)-plane, set $p_1 = p$ and return Step 2.

3.3.2 Construction C2

Fix a cross section a_M between a_L and a_R. The last part of the Riemann solution can be a stationary wave

$$W_0(U_R^s, U_R),$$

where

$$\begin{aligned} &U_R^s = \left(p_R^s, u_R^s, \rho_R^s, a_L\right), \\ &\rho_R^s := \varphi_1(U_R, a_M), \quad u_R^s := \frac{a_R \rho_R u_R}{a_M \rho_R^s}, \quad p_R^s := \kappa(S_R)(\rho_R^s)^\gamma. \end{aligned} \tag{3.11}$$

The next part of the Riemann solution can be the 3-shock wave with zero speed

$$S_3(U_R^{s@}, U_R^s).$$

The next part of the Riemann solution can be again a stationary wave

$$W_0(U_R^{s@b}, U_R^{s@}),$$

where

$$U_R^{s@b} = (p, u, \rho, a_L),$$
$$\rho := \varphi_2(U_R^{s@}, a_L), \quad u := \frac{a_M \rho_R^{s@} u_R^{s@}}{a_L \rho}, \quad p := \kappa(S_R^{s@})\rho^\gamma. \tag{3.12}$$

Because these three parts are discontinuity waves with same zero speed, we have a wave collision (resonant case), i.e., $W_0(U_R^{s@b}, U_R^{s@}) \oplus S_3(U_R^{s@}, U_R^s) \oplus W_0(U_R^s, U_R)$ is just a discontinuity wave with zero speed

$$U_{\text{Rie}}(x/t; U_L, U_R) = \begin{cases} \dots, \\ U_R^{s@b} & \text{if } \dots < x/t < 0, \\ U_R & \text{if } x/t > 0. \end{cases}$$

We call the set

$$\{U_R^{s@b} : \quad a_M \text{ varies between } a_L \text{ and } a_R\}$$

as the backward composite wave curve $W_0^B.S_3^B.W_0^B(U_R, a_L)$. It is not difficult to check that $U_R^{s@}$ and $U_R^{@b}$ are two end-points of $W_0^B.S_3^B.W_0^B(U_R, a_L)$ (see Fig. 4). If the wave curve $\mathcal{W}_1(U_L)$ intersects $W_0^B.S_3^B.W_0^B(U_R, a_L)$ at a point (p, u) in the (p, u)-plane, then the Riemann problem for (1.1) has a solution of the form

$$W_1(U_L, U^*) \oplus W_2(U^*, U_R^{s@b}) \oplus W_0(U_R^{s@b}, U_R^{s@}) \oplus S_3(U_R^{s@}, U_R^s) \oplus W_0(U_R^s, U_R), \tag{3.13}$$

where

$$U^* = (p, u, \rho^*, a_L) \in \mathcal{W}_1(U_L).$$

Explicitly, the form (3.13) can be seen as follows.

• If $U^* \in \mathcal{R}_1(U_L)$, then the form (3.13) yields

$$U_{\text{Rie}}(x/t; U_L, U_R) = \begin{cases} U_L & \text{if } x/t < \lambda_1(U_L), \\ \text{Fan}_1(x/t; U_L, U^*) & \text{if } \lambda_1 \le x/t \le \lambda_1(U_*), \\ U^* & \text{if } \lambda_1(U^*) < x/t < \lambda_2(U^*) = \lambda_2(U_R^{s@b}), \\ U_R^{s@b} & \text{if } \lambda_2(U_R^{s@b}) < x/t < 0, \\ U_R & \text{if } x/t > 0. \end{cases}$$

• If $U^* \in \mathcal{S}_1(U_L)$, then the form (3.13) yields

$$U_{\text{Rie}}(x/t; U_L, U_R) = \begin{cases} U_L & \text{if } x/t < \sigma_1(U_L, U^*), \\ U^* & \text{if } \sigma_1(U_L, U^*) < x/t < \lambda_2(U^*) = \lambda_2(U_R^{s@b}), \\ U_R^{s@b} & \text{if } \lambda_2(U_R^{s@b}) < x/t < 0, \\ U_R & \text{if } x/t > 0. \end{cases}$$

Algorithm to Compute the Intersection Point $(p, u) = \mathcal{W}_1(U_L) \cap W_0^B.S_3^B.W_0^B\ (U_R, a_L)$. Assume that $U_R^{s@}$ is located below $\mathcal{W}_1(U_L)$ and $U_R^{@b}$ is located above $\mathcal{W}_1(U_L)$ in the $(p, u)-$plane.

Step 1 Set $a_1 = a_L, a_2 = a_R$;

Step 2 Compute $a_M = \dfrac{a_1 + a_2}{2}$; Compute U_R^s as in (3.11); Compute $U_R^{s@}$; Compute $U_R^{s@b} = (p, u, \rho, a_L)$ as in (3.12);

Step 3 – If (p, u) belongs to $\mathcal{W}_1(U_L)$ in the (p, u)-plane, end;
– If (p, u) is located above $\mathcal{W}_1(U_L)$ in the (p, u)-plane, set $a_1 = a_M$ and return Step 2;
– If (p, u) is located below $\mathcal{W}_1(U_L)$ in the (p, u)-plane, set $a_2 = a_M$ and return Step 2.

3.3.3 Construction C3

Take a state $U = (p, u, \rho, a_R) \in \mathcal{S}_3^B(U_R)$ such that U is located between $U_R^{@}$ and U_R^0, where

$$U_R^0 = (p_R^0, u_R^0, \rho_R^0, a_R) = \mathcal{W}_3^B(U_R) \cap \mathcal{C}^0.$$

Then, the last part of the Riemann solution can be a 3-shock wave with positive speed

$$S_3(U, U_R),$$

(see Lemma 2.1). The next part of the Riemann solution can be a stationary wave

$$W_0(U^b, U),$$

where

$$\begin{aligned} &U^b = \left(p^b, u^b, \rho^b, a_L\right), \\ &\rho^b := \varphi_2(U, a_L), \quad u^b := \frac{a_R \rho u}{a_L \rho^b}, \quad p^b := \kappa(S)(\rho^b)^\gamma. \end{aligned} \tag{3.14}$$

We call the set

$$\{U^b : \quad U \text{ is located between } U_R^{@} \text{ and } U_R^0 \text{ on } \mathcal{S}_3^B(U_R)\}$$

as the backward composite wave curve $S_3^B.W_0^B(U_R, a_L)$. Obviously, $U_R^{@b}$ and U_R^0 are two end-points of $S_3^B.W_0^B(U_R, a_L)$ (see Fig. 4). If the wave curve $\mathcal{W}_1(U_L)$ intersects $S_3^B.W_0(U_R, a_L)$ at a point (p^b, u^b) in the (p, u)-plane, then the Riemann problem for (1.1) has a solution of the form

$$W_1(U_L, U^*) \oplus W_2(U^*, U^b) \oplus W_0(U^b, U) \oplus S_3(U, U_R), \tag{3.15}$$

where

$$U^* = (p^b, u^b, \rho^*, a_L) \in \mathcal{W}_1(U_L).$$

Explicitly, the form (3.15) can be seen as follows.
• If $U^* \in \mathcal{R}_1(U_L)$, then the form (3.15) yields

$$U_{\text{Rie}}(x/t; U_L, U_R) = \begin{cases} U_L & \text{if } x/t < \lambda_1(U_L), \\ \text{Fan}_1(x/t; U_L, U^*) & \text{if } \lambda_1 \le x/t \le \lambda_1(U_*), \\ U^* & \text{if } \lambda_1(U^*) < x/t < \lambda_2(U^*) = \lambda_2(U^b), \\ U^b & \text{if } \lambda_2(U^b) < x/t < 0, \\ U & \text{if } 0 < x/t < \sigma_3(U, U_R), \\ U_R & \text{if } x/t > \sigma_3(U, U_R). \end{cases}$$

• If $U^* \in \mathcal{S}_1(U_L)$, then the form (3.15) yields

$$U_{\text{Rie}}(x/t; U_L, U_R) = \begin{cases} U_L & \text{if } x/t < \sigma_1(U_L, U^*), \\ U^* & \text{if } \sigma_1(U_L, U^*) < x/t < \lambda_2(U^*) = \lambda_2(U^b), \\ U^b & \text{if } \lambda_2(U^b) < x/t < 0, \\ U & \text{if } 0 < x/t < \sigma_3(U, U_R), \\ U_R & \text{if } x/t > \sigma_3(U, U_R). \end{cases}$$

Algorithm to Compute the State U and the Intersection Point $(p^b, u^b) = \mathcal{W}_1(U_L) \cap S_3^B.W_0(U_R, a_L)$. Assume that $U_R^{@b}$ is located below $\mathcal{W}_1(U_L)$ and U_R^0 is located above $\mathcal{W}_1(U_L)$ in the (p, u)-plane.

Step 1 Set $p_1 = p_R^@$, $p_2 = p_R^0$;

Step 2 Compute $p = \frac{p_1+p_2}{2}$; Compute $U = (p, u, \rho, a_R) \in \mathcal{S}_3^B(U_R)$; Compute $U^b = (p^b, u^b, \rho^b, a_L)$ as in (3.14);

Step 3 – If (p^b, u^b) belongs to $\mathcal{W}_1(U_L)$ in the (p, u)-plane, end;
– If (p^b, u^b) is located above $\mathcal{W}_1(U_L)$ in the (p, u)-plane, set $p_2 = p$ and return Step 2;
– If (p^b, u^b) is located below $\mathcal{W}_1(U_L)$ in the (p, u)-plane, set $p_1 = p$ and return Step 2.

3.4 Case D: $U_R \in G_2^-$ and $a_L > a_R$

3.4.1 Construction D1

The last part of the Riemann solution can be the 3-rarefaction wave

$$R_3(U_R^-, U_R),$$

where

$$U_R^- = (p_R^-, u_R^-, \rho_R^-, a_R) = \mathcal{W}_3^B(U_R) \cap \mathcal{C}^-.$$

The next part of the Riemann solution can be the stationary wave

$$W_0(U_R^{-s}, U_R^-),$$

where

$$U_R^{-s} = \left(p_R^{-s}, u_R^{-s}, \rho_R^{-s}, a_L\right),$$
$$\rho_R^{-s} := \varphi_1(U_R^-, a_L), \quad u_R^{-s} := \frac{a_R \rho_R^- u_R^-}{a_L \rho_R^{-s}}, \quad p_R^{-s} := \kappa(S_R)(\rho_R^{-s})^\gamma.$$

Take any state $U = (p, u, \rho, a_L) \in \mathcal{W}_3^B(U_R^{-s})$ such that U is located below $U_R^{-s@}$. Then, the next part of the Riemann solution can be a 3-wave

$$W_3(U, U_R^{-s}).$$

We call the set

$$\{U \in \mathcal{W}_3^B(U_R^{-s}) : \quad U \text{ is located below } U_R^{-s@}\}$$

as the backward composite wave curve $R_3^B.W_0^B.W_3^B(U_R, a_L)$ (see Fig. 5). If the wave curve $\mathcal{W}_1(U_L)$ intersects $R_3^B.W_0^B.W_3^B(U_R, a_L)$ at a point (p, u) in the $(p, u)-$plane, then the Riemann problem for (1.1) has a solution of the form

$$W_1(U_L, U^*) \oplus W_2(U^*, U) \oplus W_3(U, U_R^{-s}) \oplus W_0(U_R^{-s}, U_R^-) \oplus R_3(U_R^-, U_R), \tag{3.16}$$

where

$$U^* = (p, u, \rho^*, a_L) \in \mathcal{W}_1(U_L).$$

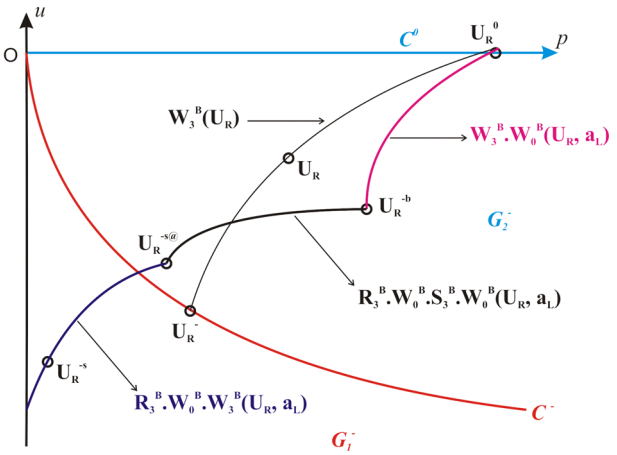

Fig. 5 The backward composite wave curves: $R_3^B.W_0^B.W_3^B(U_R, a_L)$, $R_3^B.W_0^B.S_3^B.W_0^B(U_R, a_L)$, and $W_3^B.W_0^B(U_R, a_L)$ in the (p, u)-plane

Explicitly, the form (3.16) can be seen as follows.

• If $U \in \mathcal{R}_3^B(U_R^{-s})$ and $U^* \in \mathcal{R}_1(U_L)$, then the form (3.16) yields

$$U_{\text{Rie}}(x/t; U_L, U_R) = \begin{cases} U_L & \text{if } x/t < \lambda_1(U_L), \\ \text{Fan}_1(x/t; U_L, U^*) & \text{if } \lambda_1 \le x/t \le \lambda_1(U_*), \\ U^* & \text{if } \lambda_1(U^*) < x/t < \lambda_2(U^*) = \lambda_2(U), \\ U & \text{if } \lambda_2(U) < x/t < \lambda_3(U), \\ \text{Fan}_3(x/t; U, U_R^{-s}) & \text{if } \lambda_3(U) \le x/t \le \lambda_3(U_R^{-s}), \\ U_R^{-s} & \text{if } \lambda_3(U_R^{-s}) < x/t < 0, \\ \text{Fan}_3(x/t; U_R^-, U_R) & \text{if } 0 = \lambda_3(U_R^-) \le x/t \le \lambda_3(U_R), \\ U_R & \text{if } x/t > \lambda_3(U_R). \end{cases}$$

• If $U \in \mathcal{R}_3^B(U_R^{-s})$ and $U^* \in \mathcal{S}_1(U_L)$, then the form (3.16) yields

$$U_{\text{Rie}}(x/t; U_L, U_R) = \begin{cases} U_L & \text{if } x/t < \sigma_1(U_L, U^*), \\ U^* & \text{if } \sigma_1(U_L, U^*) < x/t < \lambda_2(U^*) = \lambda_2(U), \\ U & \text{if } \lambda_2(U) < x/t < \lambda_3(U), \\ \text{Fan}_3(x/t; U, U_R^{-s}) & \text{if } \lambda_3(U) \le x/t \le \lambda_3(U_R^{-s}), \\ U_R^{-s} & \text{if } \lambda_3(U_R^{-s}) < x/t < 0, \\ \text{Fan}_3(x/t; U_R^-, U_R) & \text{if } 0 = \lambda_3(U_R^-) \le x/t \le \lambda_3(U_R), \\ U_R & \text{if } x/t > \lambda_3(U_R). \end{cases}$$

• If $U \in \mathcal{S}_3^B(U_R^{-s})$ and $U^* \in \mathcal{R}_1(U_L)$, then the form (3.16) yields

$$U_{\text{Rie}}(x/t; U_L, U_R) = \begin{cases} U_L & \text{if } x/t < \lambda_1(U_L), \\ \text{Fan}_1(x/t; U_L, U^*) & \text{if } \lambda_1 \le x/t \le \lambda_1(U_*), \\ U^* & \text{if } \lambda_1(U^*) < x/t < \lambda_2(U^*) = \lambda_2(U), \\ U & \text{if } \lambda_2(U) < x/t < \sigma_3(U, U_R^{-s}), \\ U_R^{-s} & \text{if } \sigma_3(U, U_R^{-s}) < x/t < 0, \\ \text{Fan}_3(x/t; U_R^-, U_R) & \text{if } 0 = \lambda_3(U_R^-) \le x/t \le \lambda_3(U_R), \\ U_R & \text{if } x/t > \lambda_3(U_R). \end{cases}$$

• If $U \in \mathcal{S}_3^B(U_R^{-s})$ and $U^* \in \mathcal{S}_1(U_L)$, then the form (3.16) yields

$$U_{\text{Rie}}(x/t; U_L, U_R) = \begin{cases} U_L & \text{if } x/t < \sigma_1(U_L, U^*), \\ U^* & \text{if } \sigma_1(U_L, U^*) < x/t < \lambda_2(U^*) = \lambda_2(U), \\ U & \text{if } \lambda_2(U) < x/t < \sigma_3(U, U_R^{-s}), \\ U_R^{-s} & \text{if } \sigma_3(U, U_R^{-s}) < x/t < 0, \\ \text{Fan}_3(x/t; U_R^-, U_R) & \text{if } 0 = \lambda_3(U_R^-) \le x/t \le \lambda_3(U_R), \\ U_R & \text{if } x/t > \lambda_3(U_R). \end{cases}$$

Algorithm to Compute the Intersection Point $(p, u) = \mathcal{W}_1(U_L) \cap R_3^B.W_0.W_3^B\ (U_R, a_L)$. Similar to case C, since $R_3^B.W_0^B.W_3^B(U_R, a_L) \equiv W_0^B.W_3^B(U_R^-, a_L)$.

3.4.2 Construction D2

The last part of the Riemann solution can be the 3-rarefaction wave

$$R_3(U_R^-, U_R),$$

where

$$U_R^- = (p_R^-, u_R^-, \rho_R^-, a_R) = \mathcal{W}_3^B(U_R) \cap \mathcal{C}^-.$$

Fix a cross section a_M between a_L and a_R. The next backward part of the Riemann solution can be a stationary wave

$$W_0(U_R^{-s}, U_R^-),$$

where

$$U_R^{-s} = \left(p_R^{-s}, u_R^{-s}, \rho_R^{-s}, a_M\right),$$

$$\rho_R^{-s} := \varphi_1(U_R^-, a_M), \quad u_R^{-s} := \frac{a_R \rho_R^- u_R^-}{a_M \rho_R^{-s}}, \quad p_R^{-s} := \kappa(S_R)(\rho_R^{-s})^\gamma.$$

The next backward part of the Riemann solution can be a 3-shock wave with zero speed

$$S_3(U_R^{-s@}, U_R^{-s}),$$

(see Lemma 2.1). The next backward part of the Riemann solution can be again a stationary wave

$$W_0(U_R^{-s@b}, U_R^{-s@}),$$

where

$$U_R^{-s@b} = (p, u, \rho, a_L),$$

$$\rho := \varphi_2(U_R^{-s@}, a_L), \quad u := \frac{a_M \rho_R^{-s@} u_R^{-s@}}{a_L \rho}, \quad p := \kappa(S_R^{-s@})\rho^\gamma.$$

We call the set

$$\{U_R^{-s@b}: \quad a_M \text{ varies between } a_L \text{ and } a_R\}$$

as the backward composite wave curve $R_3^B.W_0^B.S_3^B.W_0^B(U_R, a_L)$. It is not difficult to check that $U_R^{-s@}$ and U_R^{-b} are two end-points of $R_3^B.W_0^B.S_3^B.W_0^B(U_R, a_L)$ (see Fig. 5). If the wave curve $\mathcal{W}_1(U_L)$ intersects $R_3^B.W_0^B.S_3^B.W_0^B(U_R, a_L)$ at a point (p, u) in the (p, u)-plane, then the Riemann problem for (1.1) has a solution of the form

$$\begin{aligned} &W_1(U_L, U^*) \oplus W_2(U^*, U_R^{-s@b}) \oplus W_0(U_R^{-s@b}, U_R^{-s@}) \\ \oplus\ &S_3(U_R^{-s@}, U_R^{-s}) \oplus W_0(U_R^{-s}, U_R^-) \oplus R_3(U_R^-, U_R), \end{aligned} \tag{3.17}$$

where

$$U^* = (p, u, \rho^*, a_L) \in \mathcal{W}_1(U_L).$$

Explicitly, the form (3.17) can be seen as follows.

• If $U^* \in \mathcal{R}_1(U_L)$, then the form (3.17) yields

$$U_{\text{Rie}}(x/t; U_L, U_R) = \begin{cases} U_L & \text{if } x/t < \lambda_1(U_L), \\ \text{Fan}_1(x/t; U_L, U^*) & \text{if } \lambda_1 \le x/t \le \lambda_1(U_*), \\ U^* & \text{if } \lambda_1(U^*) < x/t < \lambda_2(U^*) = \lambda_2(U_R^{-s@b}), \\ U_R^{-s@b} & \text{if } \lambda_2(U_R^{-s@b}) < x/t < 0, \\ \text{Fan}_3(x/t; U_R^-, U_R) & \text{if } 0 = \lambda_3(U_R^-) \le x/t \le \lambda_3(U_R), \\ U_R & \text{if } x/t > \lambda_3(U_R). \end{cases}$$

• If $U^* \in \mathcal{S}_1(U_L)$, then the form (3.17) yields

$$U_{\text{Rie}}(x/t; U_L, U_R) = \begin{cases} U_L & \text{if } x/t < \sigma_1(U_L, U^*), \\ U^* & \text{if } \sigma_1(U_L, U^*) < x/t < \lambda_2(U^*) = \lambda_2(U_R^{-s@b}), \\ U_R^{-s@b} & \text{if } \lambda_2(U_R^{-s@b}) < x/t < 0, \\ \text{Fan}_3(x/t; U_R^-, U_R) & \text{if } 0 = \lambda_3(U_R^-) \le x/t \le \lambda_3(U_R), \\ U_R & \text{if } x/t > \lambda_3(U_R). \end{cases}$$

Algorithm to Compute the Intersection Point $(p, u) = \mathcal{W}_1(U_L) \cap R_3^B.W_0^B.S_3^B.W_0^B(U_R, a_L)$. Similar to case C, since $R_3^B.W_0^B.S_3^B.W_0^B(U_R, a_L) \equiv W_0^B.S_3^B.W_0^B(U_R^-, a_L)$.

3.4.3 Construction D3

Take a state $U = (p, u, \rho, a_R) \in \mathcal{W}_3^B(U_R)$ such that $U \in G_2^-$, i.e., U is located between U_R^- and U_R^0, where

$$U_R^- = (p_R^-, u_R^-, \rho_R^-, a_R) = \mathcal{W}_3^B(U_R) \cap \mathcal{C}^-,$$
$$U_R^0 = (p_R^0, u_R^0, \rho_R^0, a_R) = \mathcal{W}_3^B(U_R) \cap \mathcal{C}^0.$$

Then, the last part of the Riemann solution can be a 3-wave

$$W_3(U, U_R).$$

The next backward part of the Riemann solution can be a stationary wave

$$W_0(U^b, U),$$

where

$$U^b = \left(p^b, u^b, \rho^b, a_L\right),$$
$$\rho^b := \varphi_2(U, a_L), \quad u^b := \frac{a_R \rho u}{a_L \rho^b}, \quad p^b := \kappa(S)(\rho^b)^\gamma.$$

We call the set

$$\{U^b : \quad U \text{ is located between } U_R^- \text{ and } U_R^0 \text{ on } \mathcal{W}_3^B(U_R)\}$$

as the backward composite wave curve $W_3^B.W_0^B(U_R, a_L)$. Obviously, U_R^{-b} and U_R^0 are two end-points of $W_3^B.W_0^B(U_R, a_L)$ (see Fig. 5). If the wave curve $\mathcal{W}_1(U_L)$ intersects $W_3^B.W_0(U_R, a_L)$ at a point (p^b, u^b) in the (p, u)-plane, then the Riemann problem for (1.1) has a solution of the form

$$W_1(U_L, U^*) \oplus W_2(U^*, U^b) \oplus W_0(U^b, U) \oplus W_3(U, U_R), \tag{3.18}$$

where

$$U^* = (p^b, u^b, \rho^*, a_L) \in \mathcal{W}_1(U_L).$$

Explicitly, the form (3.18) can be seen as follows.
• If $U \in \mathcal{R}_3^B(U_R)$ and $U^* \in \mathcal{R}_1(U_L)$, then the form (3.18) yields

$$U_{\text{Rie}}(x/t; U_L, U_R) = \begin{cases} U_L & \text{if } x/t < \lambda_1(U_L), \\ \text{Fan}_1(x/t; U_L, U^*) & \text{if } \lambda_1 \le x/t \le \lambda_1(U_*), \\ U^* & \text{if } \lambda_1(U^*) < x/t < \lambda_2(U^*) = \lambda_2(U^b), \\ U^b & \text{if } \lambda_2(U^b) < x/t < 0, \\ U & \text{if } 0 < x/t < \lambda_3(U), \\ \text{Fan}_3(x/t; U, U_R) & \text{if } \lambda_3(U) \le x/t \le \lambda_3(U_R), \\ U_R & \text{if } x/t > \lambda_3(U_R). \end{cases}$$

• If $U \in \mathcal{R}_3^B(U_R)$ and $U^* \in \mathcal{S}_1(U_L)$, then the form (3.18) yields

$$U_{\text{Rie}}(x/t; U_L, U_R) = \begin{cases} U_L & \text{if } x/t < \sigma_1(U_L, U^*), \\ U^* & \text{if } \sigma_1(U_L, U^*) < x/t < \lambda_2(U^*) = \lambda_2(U^b), \\ U^b & \text{if } \lambda_2(U^b) < x/t < 0, \\ U & \text{if } 0 < x/t < \lambda_3(U), \\ \text{Fan}_3(x/t; U, U_R) & \text{if } \lambda_3(U) \le x/t \le \lambda_3(U_R), \\ U_R & \text{if } x/t > \lambda_3(U_R). \end{cases}$$

• If $U \in \mathcal{S}_3^B(U_R)$ and $U^* \in \mathcal{R}_1(U_L)$, then the form (3.18) yields

$$U_{\text{Rie}}(x/t; U_L, U_R) = \begin{cases} U_L & \text{if } x/t < \lambda_1(U_L), \\ \text{Fan}_1(x/t; U_L, U^*) & \text{if } \lambda_1 \le x/t \le \lambda_1(U_*), \\ U^* & \text{if } \lambda_1(U^*) < x/t < \lambda_2(U^*) = \lambda_2(U^b), \\ U^b & \text{if } \lambda_2(U^b) < x/t < 0, \\ U & \text{if } 0 < x/t < \sigma_3(U, U_R), \\ U_R & \text{if } x/t > \sigma_3(U, U_R). \end{cases}$$

• If $U \in \mathcal{S}_3^B(U_R)$ and $U^* \in \mathcal{S}_1(U_L)$, then the form (3.18) yields

$$U_{\text{Rie}}(x/t; U_L, U_R) = \begin{cases} U_L & \text{if } x/t < \sigma_1(U_L, U^*), \\ U^* & \text{if } \sigma_1(U_L, U^*) < x/t < \lambda_2(U^*) = \lambda_2(U^b), \\ U^b & \text{if } \lambda_2(U^b) < x/t < 0, \\ U & \text{if } 0 < x/t < \sigma_3(U, U_R), \\ U_R & \text{if } x/t > \sigma_3(U, U_R). \end{cases}$$

Algorithm to Compute the State U and the Intersection Point $(p^b, u^b) = \mathcal{W}_1(U_L) \cap W_3^B.W_0(U_R, a_L)$. Similar to Construction C3, but the assignment $p_1 = p_R^{@}$ in Step 1 is replaced by $p_1 = p_R^{-}$.

4 Building a van Leer-Type Numerical Scheme

Relying on the constructions of Riemann solutions in the previous section, we are now in a position to build up a van Leer-type scheme to compute the approximate solution of the Cauchy problem for (1.1). Let us set

$$U := \begin{pmatrix} \rho \\ \rho u \\ \rho e \\ a \end{pmatrix}, \quad F(U) := \begin{pmatrix} \rho u \\ \rho u^2 + p \\ u(\rho e + p) \\ 0 \end{pmatrix}, \quad H(U) := -\frac{1}{a} \begin{pmatrix} \rho u \\ \rho u^2 \\ u(\rho e + p) \\ 0 \end{pmatrix}.$$

Then, the system (1.1) can be written in the compact form

$$\partial_t U + \partial_x F(U) = H(U)\partial_x a, \quad t > 0, \quad x \in \mathbb{R}. \tag{4.1}$$

Accordingly, given the initial condition

$$U(x, 0) = U_0(x), \quad x \in \mathbb{R},$$

then, the discrete initial values $(U_j^0)_{j\in\mathbb{Z}}$ are given by

$$U_j^0 := \frac{1}{\Delta x} \int_{x_{j-1/2}}^{x_{j+1/2}} U_0(x)dx.$$

Suppose $U^n = (U_j^n)_{j\in\mathbb{Z}}$ at the time t_n is known. Recently, the Godunov-type scheme has been built as follows

$$U_j^{n+1} = U_j^n - \frac{\Delta t}{\Delta x} \Big(F(U_{\text{Rie}}(0-; U_j^n, U_{j+1}^n)) - F(U_{\text{Rie}}(0+; U_{j-1}^n, U_j^n)) \Big), \tag{4.2}$$

where $U_{\text{Rie}}(\frac{x}{t}; U_L, U_R)$ denotes the exact solution of the Riemann problem for (1.1) corresponding to the Riemann data (U_L, U_R). Now, in this paper, we build a van Leer-type scheme to compute the approximation $U^{n+1} = (U_j^{n+1})_{j\in\mathbb{Z}}$ of $U(\cdot, t_{n+1})$ as follows:

• (Reconstruction Step) From the sequence U^n, we construct a piecewise linear function $U_{\text{pl}}(x)$ defined by

$$U_{\text{pl}}(x) = U_j^n + \frac{S_j^n}{\Delta x}(x - x_j), \quad x_{j-1/2} < x < x_{j+1/2}, \quad j \in \mathbb{Z}, \tag{4.3}$$

where the slopes $S_j^n = (s_{j,1}^n, s_{j,2}^n, s_{j,3}^n, s_{j,4}^n)$ are defined by

$$\begin{aligned} S_j^n &= (U_{j+1}^n - U_j^n)\Phi(\theta_j^n), \\ \theta_j^n &= \frac{U_j^n - U_{j-1}^n}{U_{j+1}^n - U_j^n}, \\ \Phi(\theta) &= \frac{|\theta| + \theta}{1 + |\theta|}, \quad \textit{the van Leer's limiter function}. \end{aligned} \tag{4.4}$$

• (Evolution Step) We solve the Cauchy problem for (4.1) with the initial condition

$$U(x, 0) = U_{\text{pl}}(x), \quad x \in \mathbb{R}, \tag{4.5}$$

to find the solution $U(\cdot, \Delta t)$.

• (Cell-averaging Step) We project (in the sense of $\mathbb{L}^2$) the solution $U(\cdot, \Delta t)$ onto the piecewise constant functions, i.e., we set

$$U_j^{n+1} := \frac{1}{\Delta x} \int_{x_{j-1/2}}^{x_{j+1/2}} U(x, \Delta t)dx. \tag{4.6}$$

To make sure that the waves of local Riemann problems centered at $x_{j-1/2}$ and $x_{j+1/2}$ do not interact, we use the following C.F.L. condition

$$\frac{\Delta t}{\Delta x}\max\{|\lambda_k(U_j^n)| : k = 1, 2, 3\} \le \frac{1}{2}. \tag{4.7}$$

In order to derive a more explicit form of the scheme, we integrate (4.1) over the rectangle $(x_{j-1/2}, x_{j+1/2}) \times (0, \Delta t)$. We obtain

$$\int_{x_{j-1/2}}^{x_{j+1/2}} (U(x, \Delta t) - U(x, 0))dx + \int_0^{\Delta t} \left(F(U(x_{j+1/2} - 0, t)) - F(U(x_{j-1/2} + 0, t))\right) dt$$
$$= \int_{x_{j-1/2}}^{x_{j+1/2}} \int_0^{\Delta t} H(U(x, t))\partial_x a dx dt.$$

Using (4.3), (4.5), and (4.6), we get

$$\Delta x(U_j^{n+1} - U_j^n) + \int_0^{\Delta t} \left(F(U(x_{j+1/2} - 0, t)) - F(U(x_{j-1/2} + 0, t))\right) dt$$
$$= \int_{x_{j-1/2}}^{x_{j+1/2}} \int_0^{\Delta t} H(U(x, t))\partial_x a dx dt. \tag{4.8}$$

Using the midpoint rule, we write

$$\frac{1}{\Delta t}\int_0^{\Delta t} F(U(x_{j+1/2} \pm 0, t))dt = F(U(x_{j+1/2} \pm 0, \Delta t/2)) + O(\Delta t^2). \tag{4.9}$$

For approximating $F(U(x_{j+1/2} \pm 0, \Delta t/2))$, we use a predictor-corrector scheme. Following an idea of Hancock (see [17], for example), we define values $U_{j+1/2,\pm}^{n+1/2}$ at time $\Delta t/2$ by

$$\begin{aligned} U_{j+1/2,-}^{n+1/2} &= U_{j+1/2,-}^n - \frac{\Delta t}{2\Delta x}\left(F(U_{j+1/2,-}^n) - F(U_{j-1/2,+}^n)\right) \\ &\quad + \frac{\Delta t}{2\Delta x} H(U_{j+1/2,-}^n)(a_{j+1}^n - a_j^n)\Phi\left(\frac{a_j^n - a_{j-1}^n}{a_{j+1}^n - a_j^n}\right), \\ U_{j-1/2,+}^{n+1/2} &= U_{j-1/2,+}^n - \frac{\Delta t}{2\Delta x}\left(F(U_{j+1/2,-}^n) - F(U_{j-1/2,+}^n)\right) \\ &\quad + \frac{\Delta t}{2\Delta x} H(U_{j-1/2,+}^n)(a_{j+1}^n - a_j^n)\Phi\left(\frac{a_j^n - a_{j-1}^n}{a_{j+1}^n - a_j^n}\right), \end{aligned} \tag{4.10}$$

where

$$\begin{aligned} U_{j+1/2,-}^n &= U_{pl}(x_{j+1/2} - 0) = U_j^n + \frac{1}{2}S_j^n, \\ U_{j-1/2,+}^n &= U_{pl}(x_{j-1/2} + 0) = U_j^n - \frac{1}{2}S_j^n. \end{aligned} \tag{4.11}$$

Then, we solve the Riemann problem of (4.1) at the points $x_{j+1/2}$, $j \in \mathbb{Z}$ with piecewise constant initial data $U_{j+1/2,\pm}^{n+1/2}$, whose solutions are noted as usual

$$U_{\text{Rie}}\left(\frac{x - x_{j+1/2}}{t}; U_{j+1/2,-}^{n+1/2}, U_{j+1/2,+}^{n+1/2}\right).$$

The values $U(x_{j+1/2} \pm 0, \Delta t/2)$ in (4.9) are substituted by

$$U_{\text{Rie}}\left(0\pm; U^{n+1/2}_{j+1/2,-}, U^{n+1/2}_{j+1/2,+}\right).$$

Next, we approximate the right-hand side of (4.8) as follows.

$$\begin{aligned}
&\int_{x_{j-1/2}}^{x_{j+1/2}} \int_0^{\Delta t} H(U(x,t))\partial_x a dx dt \\
&\approx \Delta x \Delta t H\left(U(x_j, \Delta t/2)\right) \partial_x a(x_j, \Delta t/2) \\
&\approx \Delta x \Delta t H(U_j^{n+1/2}) \frac{a(x_{j+1/2}-0, \Delta t/2) - a(x_{j-1/2}+0, \Delta t/2)}{\Delta x} \\
&\approx \Delta t \frac{1}{2}\left(H\left(U^{n+1/2}_{j+1/2,+}\right) + H\left(U^{n+1/2}_{j-1/2,-}\right)\right)\left(a_{\text{Rie}}\left(0-; U^{n+1/2}_{j+1/2,-}, U^{n+1/2}_{j+1/2,+}\right)\right. \\
&\quad \left. - a_{\text{Rie}}\left(0+; U^{n+1/2}_{j-1/2,-}, U^{n+1/2}_{j-1/2,+}\right)\right).
\end{aligned}$$

Thus, the scheme (4.8) becomes

$$\begin{aligned}
U_j^{n+1} \;=\; & U_j^n - \frac{\Delta t}{\Delta x}\left(F(U_{\text{Rie}}(0-, U^{n+1/2}_{j+1/2,-}, U^{n+1/2}_{j+1/2,+})) - F(U_{\text{Rie}}(0+, U^{n+1/2}_{j-1/2,-}, U^{n+1/2}_{j-1/2,+}))\right) \\
& + \frac{\Delta t}{2\Delta x}\left(H(U^{n+1/2}_{j+1/2,+}) + H(U^{n+1/2}_{j-1/2,-})\right)\left(a_{\text{Rie}}\left(0-; U^{n+1/2}_{j+1/2,-}, U^{n+1/2}_{j+1/2,+}\right)\right. \\
& \left. - a_{\text{Rie}}\left(0+; U^{n+1/2}_{j-1/2,-}, U^{n+1/2}_{j-1/2,+}\right)\right).
\end{aligned} \tag{4.12}$$

The updated values $U^{n+1/2}_{j\pm 1/2,\mp}$ can be interpreted as follows:

$$\begin{aligned}
U^{n+1/2}_{j+1/2,-} &\approx U(x_{j+1/2} - 0, \Delta t/2) \\
&\approx U(x_{j+1/2} - 0, 0) + \frac{\Delta t}{2}\frac{\partial U}{\partial t}(x_{j+1/2} - 0, 0) \\
&\approx U^n_{j+1/2,-} + \frac{\Delta t}{2}\left(-\frac{\partial F(U)}{\partial x}(x_{j+1/2} - 0, 0) + H(U)\frac{\partial a}{\partial x}(x_{j+1/2} - 0, 0)\right) \\
&\approx U^n_{j+1/2,-} - \frac{\Delta t}{2}\frac{\partial F(U)}{\partial x}(x_{j+1/2} - 0, 0) \\
&\quad + \frac{\Delta t}{2\Delta x} H(U^n_{j+1/2,-})(a^n_{j+1} - a^n_j)\Phi\left(\frac{a^n_j - a^n_{j-1}}{a^n_{j+1} - a^n_j}\right) \\
&\approx U^n_{j+1/2,-} - \frac{\Delta t}{2\Delta x}\left(F(U^n_{j+1/2,-}) - F(U^n_{j-1/2,+})\right) \\
&\quad + \frac{\Delta t}{2\Delta x} H(U^n_{j+1/2,-})(a^n_{j+1} - a^n_j)\Phi\left(\frac{a^n_j - a^n_{j-1}}{a^n_{j+1} - a^n_j}\right),
\end{aligned}$$

since

$$\partial_x a(x,0) = \frac{1}{\Delta x}(a^n_{j+1} - a^n_j)\Phi\left(\frac{a^n_j - a^n_{j-1}}{a^n_{j+1} - a^n_j}\right), \quad x_{j-1/2} < x < x_{j+1/2}.$$

A similar argument can be made for $U^{n+1/2}_{j-1/2,+}$.

To complete the van Leer-type scheme (4.12), we will specify the values $U_{\text{Rie}}(0\pm; U_L, U_R)$ as follows.

Construction	$U_{\text{Rie}}(0-; U_L, U_R)$	$U_{\text{Rie}}(0+; U_L, U_R)$
A1 (3.1)	U_L	U_L^s
A2 (3.4)	U_L	$U_L^{s\#b}$
A3 (3.6)	U	U^b
B1 (3.7)	U_L^+	U_L^{+s}
B2 (3.8)	U_L^+	$U_L^{+s\#b}$
B3 (3.9)	U	U^b
C1 (3.10)	U_R^s	U_R
C2 (3.13)	$U_R^{s@b}$	U_R
C3 (3.15)	U^b	U
D1 (3.16)	U_R^{-s}	U_R^-
D2 (3.17)	$U_R^{-s@b}$	U_R^-
D3 (3.18)	U^b	U

5 Numerical Experiments

This section is devoted to numerical tests by using MATLAB. For each test, by taking $\gamma = 1.4$ and CFL = 0.5, we plot the exact solution and its approximations corresponding to the Godunov-type scheme (4.2) and the van Leer-type scheme (4.12) at $t = 0.02$.

5.1 Approximations of Smooth Stationary Solutions

Test 1 Consider the Cauchy problem for system (1.1) with the initial data given as follows:

$$U(x, 0) = (p(x), u(x), \rho(x), a(x)), \quad x \in \mathbb{R}, \tag{5.1}$$

where

$$\begin{aligned}
&a(x) = 2 + \arctan x,\\
&a(x)\rho(x)u(x) = a(0)\rho(0)u(0),\\
&\frac{(u(x))^2}{2} + h(\rho(x)) = \frac{(u(0))^2}{2} + h(\rho(0)),\\
&\frac{p(x)}{(\rho(x))^\gamma} = \frac{p(0)}{(\rho(0))^\gamma},\\
&(p(0), u(0), \rho(0)) = (3, 10, 0.2) \in G_1^+,\\
&(p(x), u(x), \rho(x)) \in G_1^+.
\end{aligned}$$

The exact solution in this test is just the smooth stationary wave

$$U(x, t) = (p(x), u(x), \rho(x), a(x)), \quad x \in \mathbb{R}, \quad t \geq 0.$$

Figure 6 displays exact solution and its approximations for the mesh sizes $h = 1/20$, $h = 1/80$ by the van Leer-type scheme (4.12). The errors and orders for different mesh sizes $h = 1/20$, $h = 1/40$, $h = 1/80$, $h = 1/160$, $h = 1/320$, $h = 1/640$, and $h = 1/1280$ are reported in Table 1. The order of accuracy in this test is close to 2.

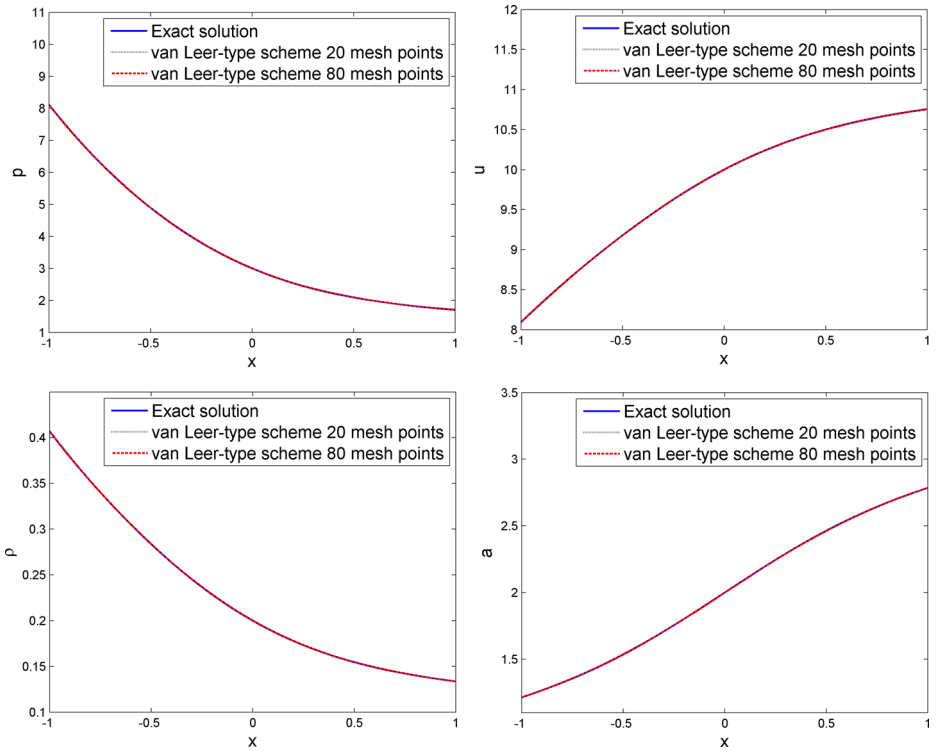

Fig. 6 Exact solution and approximate solutions for the mesh sizes $h = 1/20$ and $h = 1/80$ by the van Leer-type scheme in test 1

5.2 Test for Simple Waves

Test 2 Consider the Riemann problem for system (1.1) with the initial data given as follows

$$U(x,0) = \begin{cases} U_L = (p_L, u_L, \rho_L, a_L) = (7.0, 2.0, 0.5, 3.0) & \text{if } x < 0, \\ U_R = (p_R, u_R, \rho_R, a_R) = (7.0, 2.0, 0.4, 3.0) & \text{if } x > 0. \end{cases} \tag{5.2}$$

Table 1 Errors and orders of accuracy for test 1

	van Leer-type scheme	
N	L^1-error	L^1-order
20	0.00652770	–
40	0.00159440	2.03
80	0.00041149	1.95
160	0.00010669	1.95
320	0.00002751	1.96
640	0.00000697	1.98
1280	0.00000176	1.99

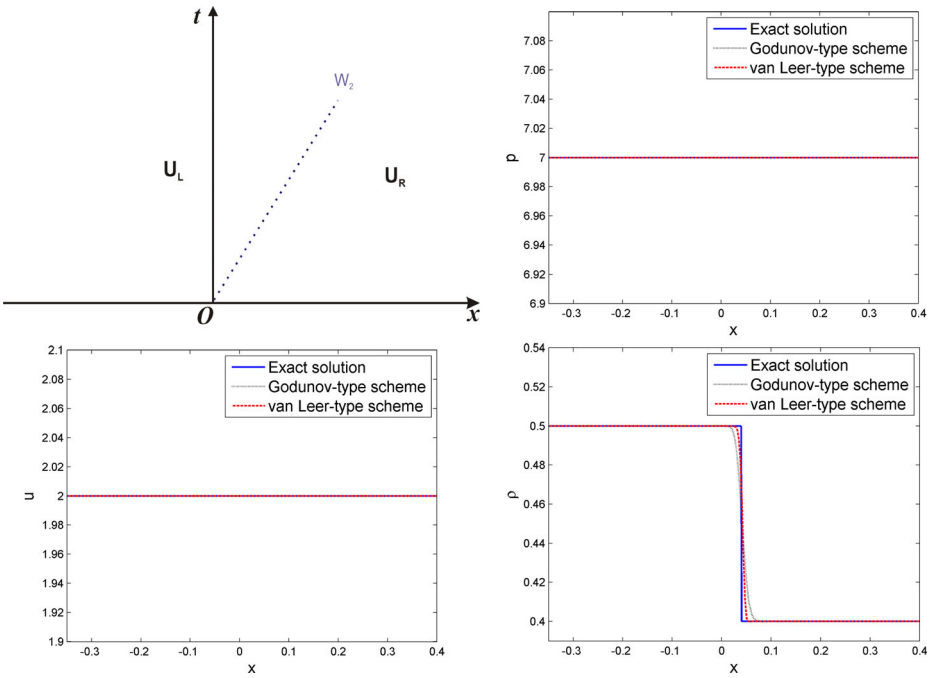

Fig. 7 Exact solution and approximate solutions for the mesh size $h = 1/640$ corresponding to the Godunov-type scheme and the van Leer-type scheme in test 2

Since $p_L = p_R, u_L = u_R$, and $a_L = a_R$, the exact solution for this test is just the 2-contact wave

$$U_{\text{Rie}}(x, t; U_L, U_R) = \begin{cases} U_L & \text{if } x < 2t, \\ U_R & \text{if } x > 2t, \end{cases}$$

see the left top of Fig. 7. Figure 7 displays exact solution and its approximations for the mesh size $h = 1/640$ corresponding to the Godunov-type scheme and the van Leer-type scheme. The errors and orders of accuracy of this test are reported in Table 2. We also evaluate from Table 2 that the L^1-order of the van Leer-type scheme is approximately equal to 0.89, while the "second-order" van Leer scheme for usual gas dynamics equations has order of accuracy approximately equal to 2/3 for contact wave. Moreover, Fig. 7 and Table 2 show

Table 2 Errors and orders of accuracy for test 2

	Godunov-type scheme		van Leer-type scheme	
N	L^1-error	L^1-order	L^1-error	L^1-order
40	0.004705	–	0.004909	–
80	0.002260	1.06	0.001576	1.64
160	0.001599	0.50	0.000881	0.84
320	0.001169	0.45	0.000646	0.45
640	0.000846	0.47	0.000442	0.55
1280	0.000583	0.54	0.000224	0.98

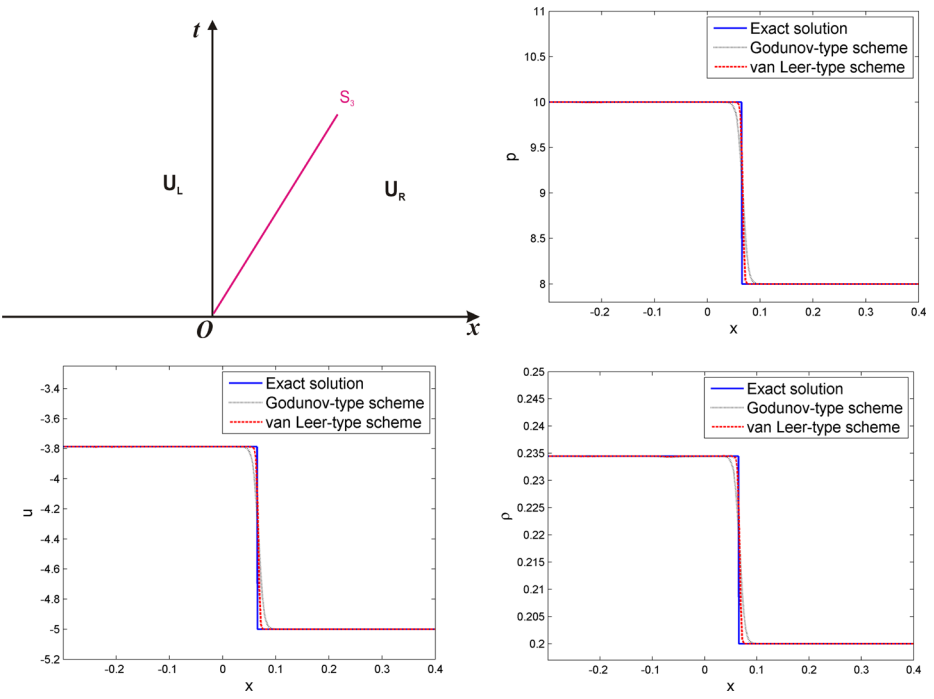

Fig. 8 Exact solution and approximate solutions for the mesh size $h = 1/640$ corresponding to the Godunov-type scheme and the van Leer-type scheme in test 3

that the accuracy and the order of accuracy of the van Leer-type scheme are better than the Godunov-type scheme.

Test 3 Consider the Riemann problem for system (1.1) with the initial data

$$U(x,0) = \begin{cases} U_L = (p_L, u_L, \rho_L, a_L) = (10.0, -3.787322, 0.234483, 2.0) & \text{if } x < 0, \\ U_R = (p_R, u_R, \rho_R, a_R) = (8.0, -5.0, 0.2, 2.0) & \text{if } x > 0. \end{cases} \tag{5.3}$$

We can check that $U_L \in \mathcal{S}_3^B(U_R)$, so the exact solution for this test is just the 3-shock wave

$$U_{\text{Rie}}(x,t;U_L,U_R) = \begin{cases} U_L & \text{if } x < \sigma_3(U_L,U_R)t, \\ U_R & \text{if } x > \sigma_3(U_L,U_R)t \end{cases}$$

Table 3 Errors and orders of accuracy for test 3

	Godunov-type scheme		van Leer-type scheme	
N	L^1-error	L^1-order	L^1-error	L^1-order
80	0.096384	–	0.075138	–
160	0.054626	0.82	0.024822	1.60
320	0.036961	0.56	0.017647	0.49
640	0.023646	0.64	0.011612	0.60
1280	0.012798	0.89	0.003850	1.59

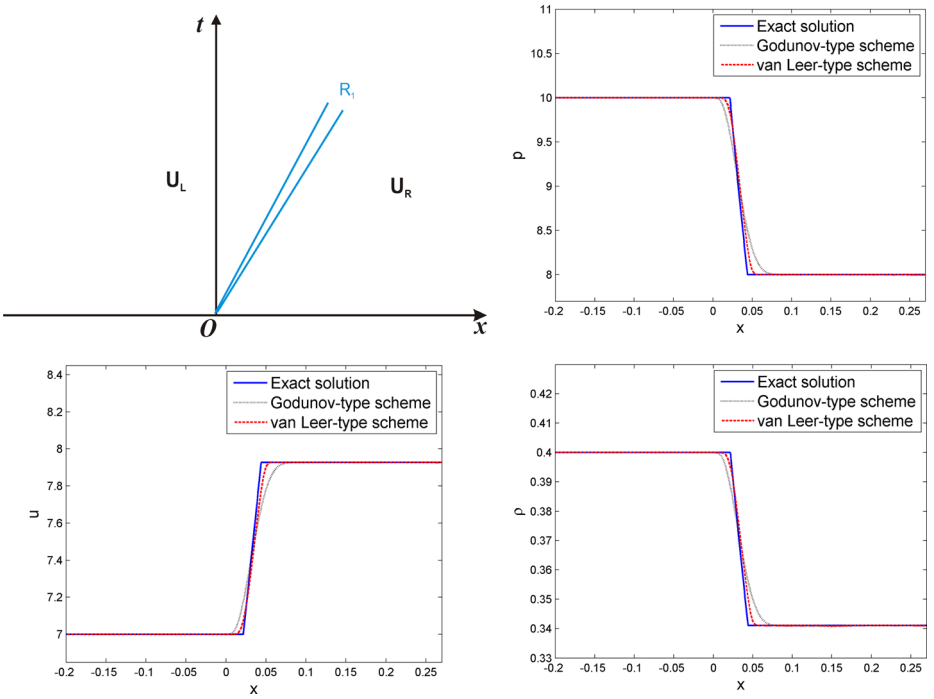

Fig. 9 Exact solution and approximate solutions for the mesh size $h = 1/640$ corresponding to the Godunov-type scheme and the van Leer-type scheme in test 4

(see the left top of Fig. 8). Figure 8 displays exact solution and its approximations for the mesh size $h = 1/640$ corresponding to the Godunov-type scheme and the van Leer-type scheme. The errors and orders of accuracy of this test are reported in Table 3. We can evaluate from Table 3 that the order is approximately equal to 1.07, while the "second-order" van Leer scheme for usual gas dynamics equations has order of accuracy approximately equal to 1.0 for shock wave. Moreover, we also see from Table 3 that the accuracy and the order of accuracy of the van Leer-type scheme are better than those of the Godunov-type scheme.

Table 4 Errors and orders of accuracy for test 4

	Godunov-type scheme		van Leer-type scheme	
N	L^1-error	L^1-order	L^1-error	L^1-order
40	0.118600	–	0.124170	–
80	0.056447	1.07	0.032811	1.92
160	0.040175	0.49	0.025166	0.38
320	0.027308	0.56	0.015104	0.74
640	0.018498	0.56	0.007769	0.96
1280	0.011947	0.63	0.003880	1.00

Table 5 States in test 5

	U^*	U^b	U
p	16.669020	16.669020	14.542474
u	−2.240080	−2.240080	−4.115752
ρ	0.702386	0.374312	0.339545
a	2.5	2.5	1.5

Test 4 Consider the Riemann problem for system (1.1) with the initial data given as follows

$$U(x,0) = \begin{cases} U_L = (p_L, u_L, \rho_L, a_L) = (10.0, 7.0, 0.4, 1.0) & \text{if } x < 0, \\ U_R = (p_R, u_R, \rho_R, a_R) = (8.0, 7.928082, 0.341066, 1.0) & \text{if } x > 0. \end{cases} \tag{5.4}$$

It is not difficult to check that $U_R \in \mathcal{R}_1(U_L)$; thus, the exact solution for this test is just the 1-rarefaction wave

$$U_{\text{Rie}}(x,t;U_L,U_R) = \begin{cases} U_L & \text{if } x < \lambda_1(U_L)t, \\ \text{Fan}_1(x/t;U_L,U_R) & \text{if } \lambda_1(U_L)t \le x \le \lambda_1(U_R)t, \\ U_R & \text{if } x > \lambda_1(U_R)t \end{cases}$$

(see the left top of Fig. 9). Figure 9 displays exact solution and its approximations for the mesh size $h = 1/640$ corresponding to the Godunov-type scheme and the van Leer-type scheme. The errors and orders of accuracy of this test are reported in Table 4. We can evaluate from Table 4 that the order is approximately equal to 1.00. This is consistent with

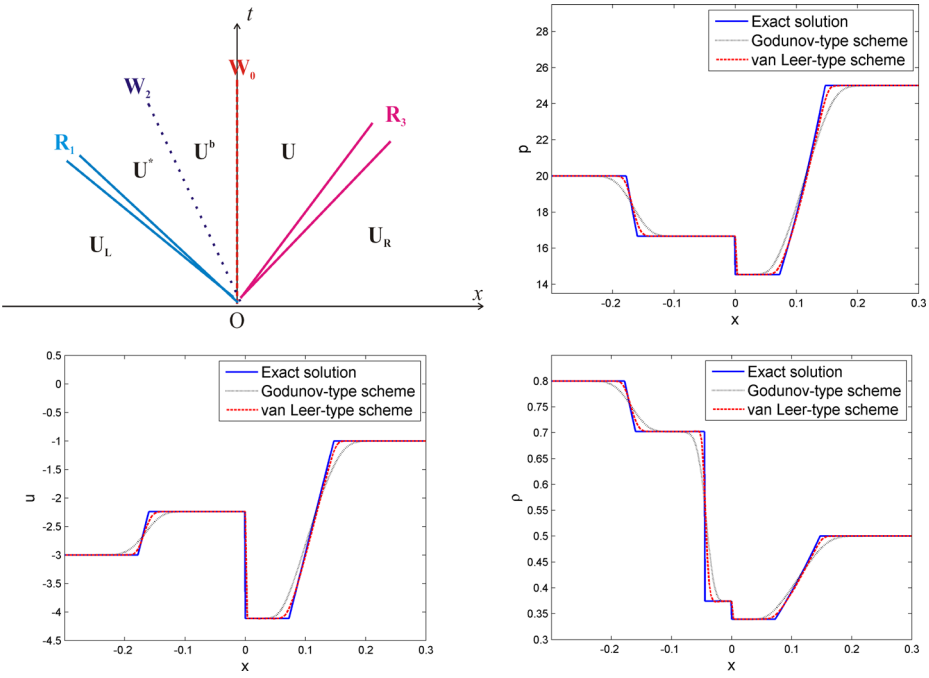

Fig. 10 Exact solution and approximate solutions for the mesh size $h = 1/640$ corresponding to the Godunov-type scheme and the van Leer-type scheme in test 5

Table 6 Errors and orders of accuracy for test 5

	Godunov-type scheme		van Leer-type scheme	
N	L^1-error	L^1-order	L^1-error	L^1-order
40	1.122100	–	0.957610	–
80	0.656010	0.77	0.435920	1.14
160	0.432860	0.60	0.228890	0.93
320	0.284290	0.61	0.117430	0.96
640	0.185340	0.62	0.060191	0.96
1280	0.117570	0.66	0.029807	1.01

the fact that the "second-order" van Leer scheme for usual gas dynamics equations has order of accuracy approximately equal to 2/3 for contact wave, and the order of accuracy is approximately equal to 1.0 for shock wave.

5.3 Tests for the Cases When Initial Data Belongs to Same Supersonic or Subsonic Region

Test 5 Let the Riemann data be given by

$$\begin{aligned} U_L &= (p_L, u_L, \rho_L, a_L) = (20.0, -3.0, 0.8, 2.5) \in G_2^-, \\ U_R &= (p_R, u_R, \rho_R, a_R) = (25.0, -1.0, 0.5, 1.5) \in G_2^-. \end{aligned} \tag{5.5}$$

The exact solution of this test is computed by Construction D3

$$R_1(U_L, U^*) \oplus W_2(U^*, U^b) \oplus W_0(U^b, U) \oplus R_3(U, U_R),$$

where U^*, U^b, and U are reported in Table 5. Figure 10 displays exact solution and its approximations for the mesh size $h = 1/640$ corresponding to the Godunov-type scheme and the van Leer-type scheme. We can see from this figure that the approximate solution corresponding to the van Leer-type scheme is closer to the exact solution than the one corresponding to the Godunov-type scheme. The errors and orders for different mesh sizes $h = 1/40$, $h = 1/80$, $h = 1/160$, $h = 1/320$, $h = 1/640$, and $1/1280$ are reported in Table 6. We can evaluate from this table that the L^1-order corresponding to the van Leer-type scheme is approximately equal to 0.98, while the one corresponding to the Godunov-type scheme is approximately equal to 0.64. So, the order of accuracy of the van Leer-type scheme is better than the one of the Godunov-type scheme.

Table 7 States in test 6

	U^*	U^b	U
p	37.348163	37.348163	32.925856
u	−2.132637	−2.132637	−3.889198
ρ	1.007640	0.874118	0.798869
a	2.5	2.5	1.5

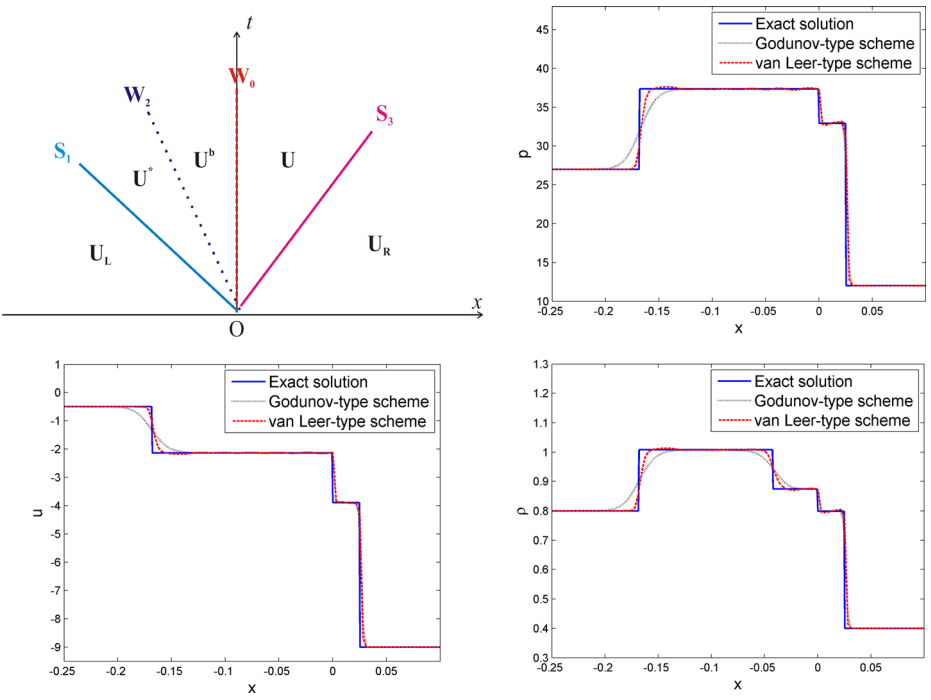

Fig. 11 Exact solution and approximate solutions for the mesh size $h = 1/640$ corresponding to the Godunov-type scheme and the van Leer-type scheme in test 6

5.4 Test Cases for Initial Data in Different Regions Without Resonance (No Wave Collisions)

Test 6 Let the Riemann data be given by

$$U_L = (p_L, u_L, \rho_L, a_L) = (27.0, -0.5, 0.8, 2.5) \in G_2^-,$$
$$U_R = (p_R, u_R, \rho_R, a_R) = (12.0, -9.0, 0.4, 1.5) \in G_1^-. \tag{5.6}$$

According to Construction C3, the exact solution is

$$S_1(U_L, U^*) \oplus W_2(U^*, U^b) \oplus W_0(U^b, U) \oplus S_3(U, U_R),$$

Table 8 Errors and orders of accuracy for test 6

	Godunov-type scheme		van Leer-type scheme	
N	L^1-error	L^1-order	L^1-error	L^1-order
40	2.059300	–	1.916200	–
80	1.451800	0.50	1.303000	0.56
160	0.660860	1.14	0.494660	1.40
320	0.367600	0.85	0.241730	1.03
640	0.203470	0.85	0.121080	1.00
1280	0.108820	0.90	0.055893	1.12

Table 9 States in test 7

	U^*	$U_R^{-s@b}$	$U_R^{-s@}$	U_R^{-s}	U_R^-
p	10.105278	10.105278	8.585095	2.968002	6.858253
u	−2.933774	−2.933774	−4.339061	−8.956347	−6.233950
ρ	0.417667	0.314994	0.280368	0.135829	0.247067
a	2.5	2.5	1.899086	1.899086	1.5

where U^*, U^b, and U are reported in Table 7. Figure 11 displays exact solution and its approximations for the mesh size $h = 1/640$ corresponding to the Godunov-type scheme and the van Leer-type scheme. The errors and orders for this test are reported in Table 8. We can see from Table 8 and Fig. 11 that the accuracy and the order of accuracy of the van Leer-type scheme are better than those of the Godunov-type scheme.

5.5 Test Cases for Resonance

Test 7 Let the Riemann data be given by

$$\begin{aligned} U_L &= (p_L, u_L, \rho_L, a_L) = (13.0, -4.0, 0.5, 2.5) \in G_2^-, \\ U_R &= (p_R, u_R, \rho_R, a_R) = (9.0, -5.0, 0.3, 1.5) \in G_2^-. \end{aligned} \tag{5.7}$$

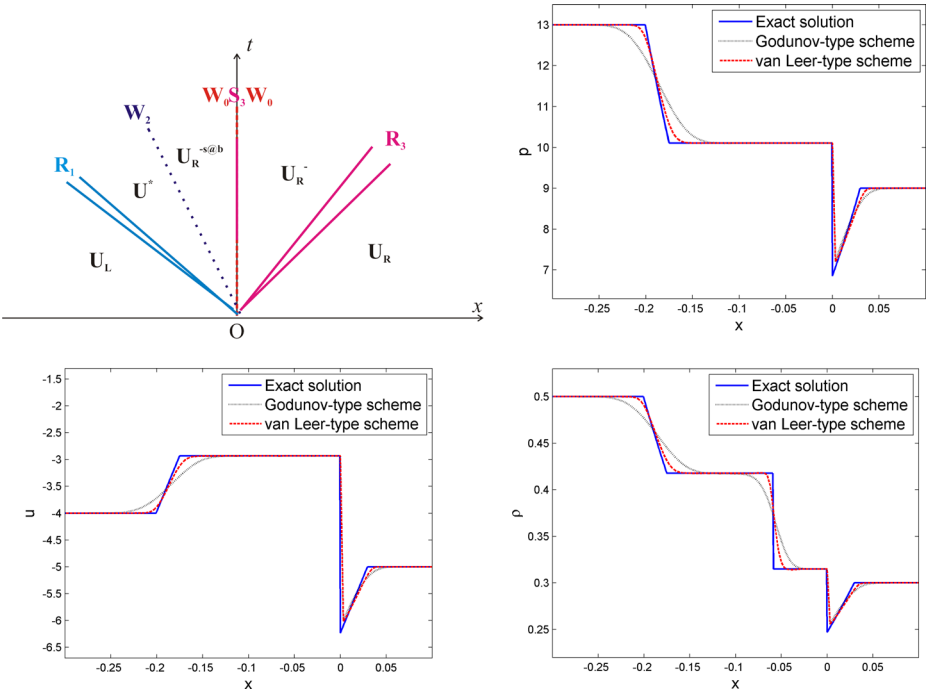

Fig. 12 Exact solution and approximate solutions for the mesh size $h = 1/640$ corresponding to the Godunov-type scheme and the van Leer-type scheme in test 7

Table 10 Errors and orders of accuracy for test 7

	Godunov-type scheme		van Leer-type scheme	
N	L^1-error	L^1-order	L^1-error	L^1-order
40	0.575220	–	0.486200	–
80	0.359630	0.68	0.276780	0.81
160	0.200990	0.84	0.135570	1.03
320	0.127810	0.65	0.071263	0.93
640	0.080678	0.66	0.036109	0.98
1280	0.051547	0.65	0.018114	1.00

The exact solution is constructed by Construction D2:

$$\begin{aligned} &R_1(U_L, U^*) \oplus W_2(U^*, U_R^{-s@b}) \oplus W_0(U_R^{-s@b}, U_R^{-s@}) \\ \oplus\ &S_3(U_R^{-s@}, U_R^{-s}) \oplus W_0(U_R^{-s}, U_R^-) \oplus R_3(U_R^-, U_R), \end{aligned}$$

where U^*, $U_R^{-s@b}$, $U_R^{-s@}$, U_R^{-s}, and U_R^- are reported in Table 9. Figure 12 displays exact solution and its approximations for the mesh size $h = 1/640$ corresponding to the Godunov-type scheme and the van Leer-type scheme. The errors and orders for different mesh sizes $h = 1/40$, $h = 1/80$, $h = 1/160$, $h = 1/320$, $h = 1/640$, and $1/1280$ are reported in Table 10. We can see from Table 10 and Fig. 12 that the accuracy and the order of accuracy of the van Leer-type scheme are better than those of the Godunov-type scheme.

6 Conclusions and Discussions

Nonconservativeness often causes lots of inconvenience for standard numerical schemes in approximating solutions. This work deals with numerical approximations of solutions of a nonconservative system. A van Leer-type scheme is built and tested. Tests show that the scheme can work through for all types of data, and of the class of high-order numerical schemes. The proposed scheme can give very desirable results for approximating exact solutions, even in the resonance cases where the exact solution may contain several waves with coinciding shock speeds. Moreover, it has a much better accuracy than the Godunov-type scheme. Note that when we deal with non-smooth solutions, a high-order scheme may give orders of accuracy below 1. Further developments for numerical approximations of solutions of more complicated systems such as multi-phase flow models will be considered.

Acknowledgements The authors are thankful to the referee for his/her very constructive comments and fruitful discussions.

Funding Information This research is funded by the Vietnam National Foundation for Science and Technology Development (NAFOSTED) under grant number 101.02-2016.15.

References

1. Ambroso, A., Chalons, C., Coquel, F., Galié, T.: Relaxation and numerical approximation of a two-fluid two-pressure diphasic model. Math. Mod. Numer. Anal. **43**, 1063–1097 (2009)
2. Ambroso, A., Chalons, C., Raviart, P.-A.: A Godunov-type method for the seven-equation model of compressible two-phase flow. Comput. Fluids **54**, 67–91 (2012)
3. Audusse, E., Bouchut, F., Bristeau, M.-O., Klein, R., Perthame, B.: A fast and stable well-balanced scheme with hydrostatic reconstruction for shallow water flows. SIAM J. Sci. Comput. **25**, 2050–2065 (2004)
4. Ben-Artzi, M., Falcovitz, J.: Generalized Riemann Problems: from the Scalar Equation to Multidimensional Fluid Dynamics Recent Advances in Computational Sciences, vol. 1–49. World Sci. Publ., Hackensack (2008)
5. Bermúdez, A., López, X.L., Vázquez-Cendón, M.E.: Numerical solution of non-isothermal non-adiabatic flow of real gases in pipelines. J. Comput. Phys. **323**, 126–148 (2016)
6. Bernetti, R., Titarev, V.A., Toro, E.F.: Exact solution of the Riemann problem for the shallow water equations with discontinuous bottom geometry. J. Comput. Phys. **227**, 3212–3243 (2008)
7. Bouchut, F.: Nonlinear Stability of Finite Volume Methods for Hyperbolic Conservation Laws, and Well-Balanced Schemes for Sources. Frontiers in Mathematics Series, Birkhäuser (2004)
8. Botchorishvili, R., Perthame, B., Vasseur, A.: Equilibrium schemes for scalar conservation laws with stiff sources. Math. Comput. **72**, 131–157 (2003)
9. Botchorishvili, R., Pironneau, O.: Finite volume schemes with equilibrium type discretization of source terms for scalar conservation laws. J. Comput. Phys. **187**, 391–427 (2003)
10. Castro, C.E., Toro, E.F.: A Riemann solver and upwind methods for a two-phase flow model in non-conservative form. Internat. J. Numer. Methods Fluids **50**, 275–307 (2006)
11. Cuong, D.H., Thanh, M.D.: A Godunov-type scheme for the isentropic model of a fluid flow in a nozzle with variable cross-section. Appl. Math. Comput. **256**, 602–629 (2015)
12. Cuong, D.H., Thanh, M.D.: Building a Godunov-type numerical scheme for a model of two-phase flows. Comput. Fluids **148**, 69–81 (2017)
13. Cuong, D.H., Thanh, M.D.: A well-balanced van Leer-type numerical scheme for shallow water equations with variable topography. Adv. Comput. Math. https://doi.org/10.1007/s10444-017-9521-4
14. Cuong, D.H., Thanh, M.D.: Constructing a Godunov-type scheme for the model of a general fluid flow in a nozzle with variable cross-section. Appl. Math. Comput. **305**, 136–160 (2017)
15. Cuong, D.H., Thanh, M.D.: A high-resolution van Leer-type scheme for a model of fluid flows in a nozzle with variable cross-section. J. Korean Math. Soc. **54**(1), 141–175 (2017)
16. Dal Maso, G., LeFloch, P.G., Murat, F.: Definition and weak stability of nonconservative products. J. Math. Pures Appl. **74**, 483–548 (1995)
17. Godlewski, E., Raviart, P.A.: Numerical Approximation of Hyperbolic Systems of Conservation Laws. Springer, New York (1996)
18. Hou, T.Y., LeFloch, P.G.: Why nonconservative schemes converge to wrong solutions. Error Anal. Math. Comput. **62**, 497–530 (1994)
19. Isaacson, E., Temple, B.: Nonlinear resonance in systems of conservation laws. SIAM J. Appl. Math. **52**, 1260–1278 (1992)
20. Isaacson, E., Temple, B.: Convergence of the 22 Godunov method for a general resonant nonlinear balance law. SIAM J. Appl. Math. **55**, 625–640 (1995)
21. Kröner, D., Thanh, M.D.: Numerical solutions to compressible flows in a nozzle with variable cross-section. SIAM J. Numer. Anal. **43**, 796–824 (2005)
22. Kröner, D., LeFloch, P.G., Thanh, M.D.: The minimum entropy principle for fluid flows in a nozzle with discntinuous crosssection. Math. Mod. Numer. Anal. **42**, 425–442 (2008)
23. LeFloch, P.G.: Shock waves for nonlinear hyperbolic systems in nonconservative form. Institute Math. Appl., Minneapolis. Preprint **593** (1989)
24. LeFloch, P.G., Thanh, M.D.: The Riemann problem for fluid flows in a nozzle with discontinuous cross-section. Comm. Math. Sci. **1**, 763–797 (2003)
25. LeFloch, P.G., Thanh, M.D.: The Riemann problem for shallow water equations with discontinuous topography. Comm. Math. Sci. **5**, 865–885 (2007)
26. LeFloch, P.G., Thanh, M.D.: A Godunov-type method for the shallow water equations with variable topography in the resonant regime. J. Comput. Phys. **230**, 7631–7660 (2011)
27. Marchesin, D., Paes-Leme, P.J.: A Riemann problem in gas dynamics with bifurcation. Hyperbolic partial differential equations III. Comput. Math. Appl. (Part A) **12**, 433–455 (1986)

28. Rosatti, G., Begnudelli, L.: The Riemann Problem for the one-dimensional, free-surface shallow water equations with a bed step: theoretical analysis and numerical simulations. J. Comput. Phys. **229**, 760–787 (2010)
29. Schwendeman, D.W., Wahle, C.W., Kapila, A.K.: The Riemann problem and a high-resolution Godunov method for a model of compressible two-phase flow. J. Comput. Phys. **212**, 490–526 (2006)
30. Saurel, R., Abgrall, R.: A multi-phase Godunov method for compressible multifluid and multiphase flows. J. Comput. Phys. **150**, 425–467 (1999)
31. Tian, B., Toro, E.F., Castro, C.E.: A path-conservative method for a five-equation model of two-phase flow with an HLLC-type Riemann solver. Comput. Fluids **46**, 122–132 (2011)
32. Thanh, M.D.: The Riemann problem for a non-isentropic fluid in a nozzle with discontinuous cross-sectional area. SIAM J. Appl. Math. **69**, 1501–1519 (2009)
33. Thanh, M.D.: A phase decomposition approach and the Riemann problem for a model of two-phase flows. J. Math. Anal. Appl. **418**, 569–594 (2014)
34. Thanh, M.D., Cuong, D.H.: Existence of solutions to the Riemann problem for a model of two-phase flows. Elect. J. Diff. Eqs. **2015**(32), 1–18 (2015)